


REVISION HISTORY			
REV	DESCRIPTION OF CHANGE	DATE	APPROVED
-	AS RELEASED	5/04/2010	
1	Component placement updated Mass budget modified (40 lbs lighter) FEA models re-solved Hand calculations: floor loading, bending, tension, and shear due to overturning moment of chassis	5/29/2010	

SIGNATURES		DATE		 <b>Zero-g ElectroStatic Thruster Testbed Reflight</b> Student Space System Fabrication Laboratory Ann Arbor, Michigan			
ENG (AUTHOR)				<h2 style="text-align: center;">STRESS ANALYSIS REPORT</h2>			
CH (CHECKER)							
APP (APPROVER)							
STRESS (NASA)							
AUTH (NASA)							
				SIZE A	CAGE CODE	REPORT NO	REV -
				SCALE: NONE		ORG	SHEET: 1 OF 51

## Table of Contents

Nomenclature .....	3
1.0 Executive Summary .....	3
2.0 Minimum Margin of Safety Summary Table.....	5
3.0 Introduction.....	9
4.0 Material Properties and Allowables.....	9
5.0 Coordinate Systems .....	10
6.0 Loads summary .....	11
7.0 Calculations.....	16
7.1 Hand Calculations .....	16
7.1.1 Cross-Section Dimension Calculations (page 29-30).....	16
7.1.2 Stress on aircraft mounting bracket (page 35).....	16
7.1.3 Floor Fittings (page 36) .....	17
7.1.3 Loads on Bolts due to Overturning Reaction Forces (page 31-32) .....	17
7.1.4 Bending, Tension, and Shear due to Overturning Reaction Forces (pages 33-34) .....	18
7.1.5 Beam Calculations .....	18
7.1.6 “Kick Loads” and Impact Analysis.....	18
7.2 FEA Analysis .....	19
7.2.1 Load Application .....	19
7.2.2 Boundary Conditions and Material Specifications.....	20
7.2.2 Mesh Strategy .....	20
7.2.3 Worst Case Scenarios .....	20
7.2.4 Scroll Pump Contingency .....	22
7.3 Modal Analysis .....	24
8.0 References .....	26
9.0 Appendices.....	27
9.1 Mass Budget.....	27
9.2 Hand Calculations .....	29
9.2 Chassis Stresses, Deflections, and Factors of Safety Under All Accelerations .....	38

## Nomenclature

d	Deformation (mm)
E	Elastic Modulus (MPa)
F	Point Load (N)
F.S.	Factor of Safety
g	gravitational acceleration ( $9.8 \text{ m/s}^2$ )
I	Moment of Inertia ( $\text{kg}\cdot\text{m}^2$ )
L	Length of the Beam (m)
$\sigma$	Stress due to Bending
M.S. <sub>ultimate</sub>	Margin of Safety (Ultimate)
M.S. <sub>yield</sub>	Margin of Safety (Yield)
$\sigma_{\text{limit}}$	Maximum Stress (MPa)
$\sigma_{\text{ultimate}}$	Ultimate Strength (MPa)
$\sigma_{\text{yield}}$	Yield Stress (MPa)

### 1.0 Executive Summary

Structural analysis was performed on the chassis beam structure, vacuum base plate, aircraft mounting brackets, and thruster mounting rod for University of Michigan's Zero-g Electrostatic Thruster Testbed (ZESTT). A combination of finite element analysis (FEA) and hand calculations using simplified and linearized equations of elastic mechanics of materials was used to determine the maximum stresses, deformations, and worst-case factors of safety. The entire experiment will not exceed 400 lbs of weight. The supporting area footprint of our experiment is 9.83 square feet; thus, the aircraft floor will not exceed 40.6 pounds per square foot.

The total weight of our chassis is 350.3 lbs with contingency. Structural verification was performed using a combination of hand calculations and finite element analysis using ANSYS WorkBench. The accelerations used matched NASA requirements: 9g forward, 6g down, 3g aft, 2g up and 2g lateral. FEA analysis and hand calculations of the chassis beam structure produced reasonable agreements between analytical and computational methods and showed a minimum factor of safety in the chassis of 2.2861 located on the side beams of the bottom plane during 6g

acceleration. FEA analysis of the thruster mounting rod and vacuum chamber mounting plate yielded factor of safety values of 3.2 and 5.1 respectively. In the worst case 9g loading, the load bearing 1515-lite beams maintain a factor of safety of 11.9, validating the FEA approximation as a concentrated point mass. The beams then, apply forces in tension and in shear to the L-brackets and bolts joining the 1515-Lite beams to the side beams of the chassis. The factor of safety of 8 is well above the limit of 2 specified by NASA.

Hand calculations of the aircraft mounting fasteners produced a worst-case factor of safety of approximately 3.8 located at the joint between the chassis and the aircraft fastener. Loading on the 727 aircraft floor will not exceed 3000 lbs with a factor of safety of 3.4. Most of the worst-case scenarios were found at the acceleration of 6g downward.

The worst-case stresses of our chassis occurred on the side beams of the base plane. All beams are connected using 6105-T5 aluminum L-brackets and a combination of 5/16"-18 and 1/4"-20 steel bolts. Physical analysis of the bottom joints has verified a sound structure and all joints will be inspected for proper positioning and tension prior to flight.

Because of the thruster's extreme positional sensitivity, modal analysis was conducted to provide a picture of the thruster mounting rod's response to dynamic and oscillatory loads. This is primarily to provide a glimpse of the worst-case deformations of the thrusters in the event the bushings fail. Using ANSYS Workbench, deformation plots were provided for the first few natural frequencies, which were also computed using Workbench.

Experimental verification was also performed for "kick loads" of 125 lbf over a 2" radius and impacts of 180 lbf at 2ft/s on the chassis structure and surrounding plastic wrap. The current structural configuration complies with NASA-specified worst case loading scenarios and has a minimum factor of safety above 2.

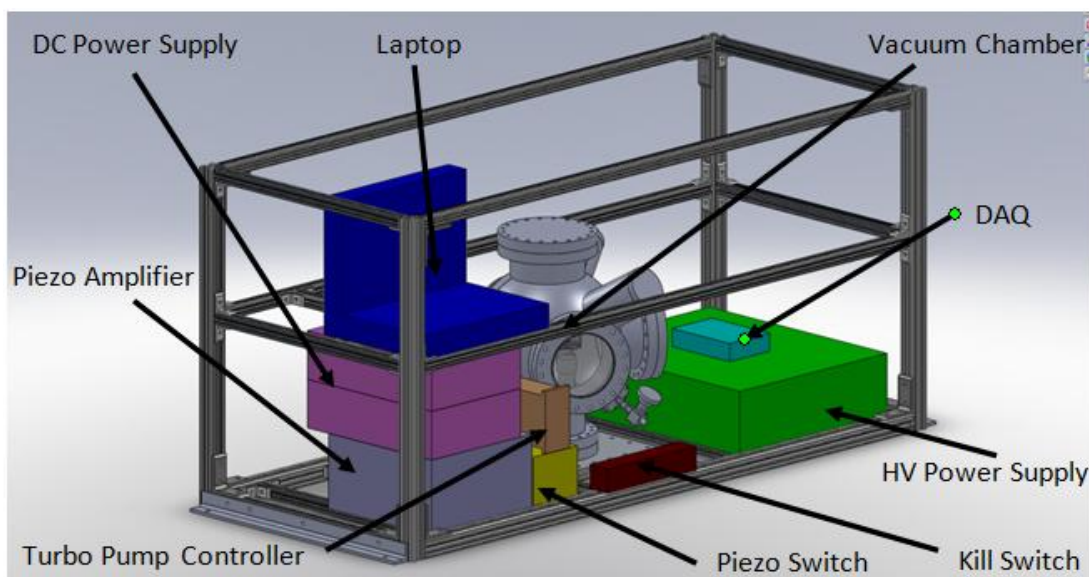


Figure 1. Proposed chassis and component placement.

## 2.0 Minimum Margin of Safety Summary Table

This report deals with all analytical, computational, and experimental measures to ensure the structural integrity of the ZESTT chassis structure and vacuum chamber components. The analysis consists of hand calculations of important structural components including beams and bolts using theorems of structural mechanics, lab testing of the plastic wrap, and finite element analysis (FEA) of the chassis, vacuum support plate, and thruster mount using ANSYS Workbench 12.5. Its goal is to prove that the minimum safety requirements detailed by NASA, namely a minimum factor of safety of 2, are met for all components of the chassis under all reasonable worst case acceleration loading scenarios specified by NASA. These consist of 9g forward, 3g aft, 6g down, 2g up, and 2g lateral loads. Its scope also includes dynamic loads of 180 lbf at 2 ft/s and 125 lbf over a 2" radius on the metal components of the chassis and the plastic wrap that safely encloses the chassis.

The applied loads on each beam are the sum of the beam weight and components on top of the beam. The detailed calculations can be found in the Appendix, section 9.2. The max stress,  $\sigma_{limit}$  was calculated as shown in section 7.1: Hand Calculations. It is the absolute maximum stress experienced by an individual beam in any single acceleration field. The yield strength of 6061 aluminum is given as 241 Pa while the ultimate strength is 290 Pa.

Margins of Safety provide a measure of how much additional load capacity the structural components can endure. Yield Margin of Safety provides a measure of how far below the yield stress the loaded structure is while the ultimate margin of safety measures how far below the ultimate strength the structure is. Yield margins of safety above 1 and Ultimate margins above 0 indicate a safe loading setup. As the following table shows, all structural components have passed the margins of safety criteria.

Sample equations for calculating the margins of safety

$$M.S._{yield} = \frac{\sigma_{yield}}{\sigma_{limit}} - 1 = \frac{241}{26.42} - 1 = 8.12 \quad (1)$$

$$M.S._{ultimate} = \frac{\sigma_{ultimate}}{\sigma_{limit} * F.S.} - 1 = \frac{290}{26.42 * 2} - 1 = 4.49 \quad (2)$$

Description		Analysis			Minimum Margin of Safety				Reference	
Part Description	Material	Failure Theory	Total Applied Load in lbs (1g)	Maximum Load Case	Yld. <sup>1</sup>	Ult. <sup>2</sup>	Max Stress (MPa)	Maximum Deflection (μm)	FEA Filenames	Report Page #s)
Vacuum Chamber Mount Plate	6061 Aluminum Alloy	Von-Mises	174.00	9-g forward	4.01	2.01	48.2	18.16	mounting_plate.wbpj	29, 40
Thruster Mount Rod	304 Stainless Steel	Von-Mises	20.00	9-g forward	2.22	1.31	64.7	780	.Mount_Post_Long.prt	19
Aircraft Mounting Bracket	6061 Aluminum Alloy	Von-Mises	390.4	9-g forward	3.8	2.0	72.3			30
1010 (56 in) Top Front	6061 Aluminum Alloy	Von-Mises	2.42	9-g forward	8.12	4.49	26.4	50.60	point_mass_model.wbpj	31
1010 (56 in) Top Back	6061 Aluminum Alloy	Von-Mises	2.42	9-g forward	8.12	4.49	26.4	50.60	point_mass_model.wbpj	31
1010 (21 in) Top Left	6061 Alumn. Alloy	Von-Mises	0.94	9-g forward	61.44	36.56	3.86	1.04	point_mass_model.wbpj	31
1010 (21 in) Top Right	6061 Alumn. Alloy	Von-Mises	0.94	9-g forward	61.44	36.56	3.86	1.04	point_mass_model.wbpj	31
1010 (56 in) Middle Back	6061 Alumn. Alloy	Von-Mises	2.42	9-g forward	8.12	4.49	26.42	50.60	point_mass_model.wbpj	31
1010 (21 in) Middle Right	6061 Alumn. Alloy	Von-Mises	0.94	9-g forward	61.44	36.56	3.86	1.04	point_mass_model.wbpj	31
1010 (21 in) Middle Left	6061 Alumn. Alloy	Von-Mises	0.94	9-g forward	61.44	36.56	3.86	1.04	point_mass_model.wbpj	31
1010 (21 in) Bottom Right	6061 Alumn. Alloy	Von-Mises	12.29	9-g forward	6.23	3.35	33.35	1.04	point_mass_model.wbpj	31
1010 (21 in) Bottom Left	6061 Alumn. Alloy	Von-Mises	36.89	9-g forward	1.41	0.45	100.10	1.04	point_mass_model.wbpj	31

1010 (21 in) Bottom	6061 Alumn. Alloy	Von- Mises	12.27	9-g forward	6.23	3.35	33.35	1.04	point_mass_model.wbpj	31
1010 (21 in) Bottom	6061 Alumn. Alloy	Von- Mises	36.89	9-g forward	1.41	0.45	100.10	1.04	point_mass_model.wbpj	31
1515 (56 in) Bottom Front	6061 Alumn. Alloy	Von- Mises	5.87	9-g forward	16.97	9.81	13.41	156.69	point_mass_model.wbpj	31
1515 (56 in) Bottom Back	6061 Alumn. Alloy	Von- Mises	10.07	9-g forward	13.47	7.71	16.65	156.69	point_mass_model.wbpj	31
1515 (21 in) Bottom Left	6061 Alumn. Alloy	Von- Mises	2.43	9-g forward	23.34	13.64	9.90	4.12	point_mass_model.wbpj	31
1515 (21 in) Bottom Right	6061 Alumn. Alloy	Von- Mises	2.43	9-g forward	23.34	13.64	9.90	4.12	point_mass_model.wbpj	31
1515 (28 in) Vertical Beam	6061 Alumn. Alloy	Von- Mises	2.53	9-g forward	75.05	44.76	3.17	10.18	point_mass_model.wbpj	31
1515 (28 in) Vertical Beam	6061 Alumn. Alloy	Von- Mises	2.53	9-g forward	75.05	44.76	3.17	10.18	point_mass_model.wbpj	31
1515 (28 in) Vertical Beam	6061 Alumn. Alloy	Von- Mises	2.53	9-g forward	75.05	44.76	3.17	10.18	point_mass_model.wbpj	31
1515 (28 in) Vertical Beam	6061 Alumn. Alloy	Von- Mises	2.53	9-g forward	75.05	44.76	3.17	10.18	point_mass_model.wbpj	31
1530 (21 in) Bottom Left	6061 Alumn. Alloy	Von- Mises	51.45	9-g forward	13.09	7.48	17.10	4.51	point_mass_model.wbpj	31
1530 (21 in) Bottom Right	6061 Alumn. Alloy	Von- Mises	51.45	9-g forward	13.09	7.48	17.10	4.51	point_mass_model.wbpj	31
1515 (21 in) Bottom Front	6061 Alumn. Alloy	Von- Mises	51.31	9-g forward	6.57	3.56	31.82	8.26	point_mass_model.wbpj	31
1515 (21 in) Bottom Back	6061 Alumn. Alloy	Von- Mises	51.31	9-g forward	6.57	3.56	31.82	8.26	point_mass_model.wbpj	31
1010 (21 in) Middle	6061 Alumn.	Von-	5.70	9-g forward	14.59	8.38	15.46	1.04	point_mass_model.wbpj	31

Inside C	Alloy	Mises								
1010 (21 in) Middle Inside C	6061 Alumn. Alloy	Von- Mises	5.70	9-g forward	14.59	8.38	15.46	1.04	point_mass_model.wbpj	31
1010 (21 in) Bottom Support	6061 Alumn. Alloy	Von- Mises	3.34	9-g forward	25.57	14.99	9.07	1.04	point_mass_model.wbpj	31

Note: Refer to Section 7.1 for hand calculations of beam stress and the Appendix for hand written calculations for vacuum plate. The stresses and deflections for thruster mount rod and vacuum chamber plate were obtained through FEA. All individual beams were hand calculated. The integrated chassis is analyzed in detail in section 7.2.

### 3.0 Introduction

This stress analysis report prepared for ZESTT details all the methods used to verify the structural integrity of the entire ZESTT structure including the chassis beams, aircraft fasteners, vacuum chamber mount plate, and thruster mount rod. The purpose of the report is to verify that the current structural configuration complies with NASA-specified worst case loading scenarios and has a minimum factor of safety above 2.

This chassis structure and vacuum base were safely flown in June 2009 as part of the ZESTT campaign at 340 lbs. This year's additional component weight has amounted to a total of 350.2 lbs with contingency. We have obtained a 100lb mass waiver for the June 17 flight week. To account for the added mass, we have lengthened and thickened the aircraft mounting brackets and analyzed the chassis structure under the appropriate acceleration fields to verify our chassis does indeed comply with NASA requirements.

### 4.0 Material Properties and Allowables

Our structural analysis is primarily concerned with the prevention of yielding. Exceeding the yield strength causes permanent plastic deformation, which is unacceptable for our application as it would compromise the safety of our chassis and irreversibly deform the testbed for future use. Therefore, all subsequent calculations of margin of safety will be performed using the yield strength as a point of reference not the ultimate tensile strength or fracture strength.

The chassis is built from three types of 6105-T5 beams differentiated by their cross-sections: 1.5" by 1.5" 1515-Lite beams serve as the four vertical and bottom perimeter beams; the thicker 1.5" by 3" 1530 beams support the vacuum chamber with their increased girth; and the slender 1" by 1" beams provide further support to the chassis on the middle perimeter and lower interior sections. These 6105-T5 beams have an Elastic Modulus of yield stress of 241 MPa.



Figure 2: 80/20 beam cross section

The vacuum support plate is made of 6061 T6 aluminum and is 3/8" thick. It bears the full brunt of the vacuum chamber weight and acceleration loads and is supported by two 1530 and two 1515-Lite beams. T6 Aluminum has an Elastic Modulus of 70 GPa and a yield stress of 275

MPa, making it better suited than other alloys to withstand the large loads of the vacuum chamber and flanges. The aircraft mounting brackets are cut from angled aluminum and span the width of the chassis base. They are made from 6061 aluminum alloy, which has the same material properties as above. The thruster mount rod is made from a 304 stainless steel hexagonal rod. It is 7/8" thick with 1/2" length sides. 304 Stainless has an E of 193 GPa and a yield stress of 205 MPa.

## 5.0 Coordinate Systems

Because all calculations and computer analyses were performed for straight beams under a number of simplifying assumptions, namely using the plane sections remain plane and infinitesimal strain theory, it is reasonable to use the right-handed Cartesian coordinate system. These coordinates permit a more simplified version of the Euler-Bernoulli beam equations explained in further detail in the Calculations section of our report. This system is also much more useful considering the nearly perfectly rectilinear configuration of the chassis beams, in which each individual beam is either perfectly perpendicular or parallel to the other beams.

The chassis beams are aligned so that they are all parallel to one axis and perpendicular to the other two. In Figure 1 for example, the longest, vertical, and shortest beams are all parallel to the y (green), z (blue), and x (red) axes respectively while remaining perpendicular to their non-parallel axes. This assumption is found to be valid even under maximal loading conditions, because of the small displacements and strains (with maximum strains usually on the order  $10^{-6}$ ) they subject the beams to.

Because the aircraft surface will be parallel to the axes of the bottom and shortest beams and normal to the axes of the vertical beams, the aircraft coordinate system will also be the identical Cartesian system of the chassis. Referring again to Figure 3, the aircraft surface will be coincident with the xy plane.

In hand calculations, when referring to specific beams, the orientation is viewed looking in the direction of the negative x-axis, as seen in all figures. The "front" is dictated by the positive x-axis while "left" and "right" dictates positive and negative y-axis directions. "Bottom" beams are in the most positive z-direction, i.e. down.

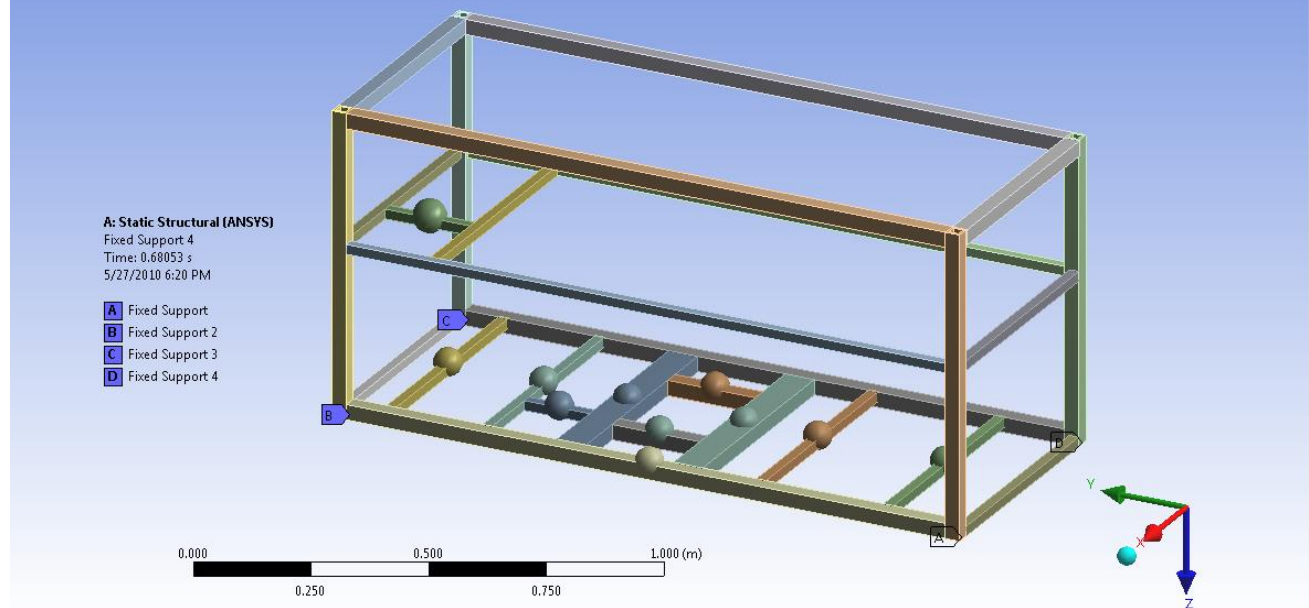


Figure 3. Orientation of the chassis with respect to the Cartesian coordinates. Fixed supports on four corners

## 6.0 Loads summary

The four corners of the chassis are defined as fixed supports to the aircraft hull while the rest of the chassis is free to deflect. The total loads of the beams include their own distributed weights and the point masses of components resting on them. We replaced these distributed component loads with point loads as a simplifying assumption. Because point loads are concentrated over an infinitesimal area and create higher stress than distributed loads, they represent the worst case loading scenario. If FEA analysis meets the factor of safety criterion using point loads, then structural integrity will be ensured for distributed loads. Acceleration loads on the individual beam weight, however, will still be represented as distributed loads through of the global accelerations option provided in Workbench.

All the beams are assumed to be of uniform density, constant cross-section extrusions, both for the FEA analysis model and the actual beam. The resulting center of mass is located at the center of the cross-section and at the midway point of the beam. For all gravity loads on the beams, point loads acting at the center of mass of these beams are replaced by distributed loads.

Table 1 outlines the component weight in pounds (in 1g) and mass acting on the chassis. Each set of tags as shown in the free body diagram represents a system of masses that act on different positions of individual beams. The bubbles on Figures 4 through 8 represent point loads due to

the masses of the chassis components such as the vacuum chamber, piezoelectric amplifier, and HV power supply box, while the yellow arrow represents a global acceleration vector, (i.e. 9g lateral acceleration loads and 6g downward acceleration loads). Chassis beam weight is already integrated into the ANSYS model and automatically factors into the ANSYS solver.

Table 1: Component Weight and Mass Positioning

Position	Description	Load (lbs.) in 1g	Component Mass (kg)
A	Acceleration Field	Varies	Varies
B	Vacuum Chamber	42.1	18.90
C	Vacuum Chamber	42.1	18.90
D	Vacuum Chamber	42.1	18.90
E	Vacuum Chamber	42.1	18.90
F	HV Power Supply DAQs and Grounding Rod	14.5	6.57
G	HV Power Supply DAQs and Grounding Rod	14.5	6.57
H	Piezo Amplifier, DC Power Supply, and Gauge Controller	29.5	13.40
I	Piezo Amplifier, DC Power Supply	26.1	11.90
J	Piezo Switch Box	2.6	1.17
K	Master Kill Switch and Wires	2.0	0.90
L	Laptop	9.4	4.23

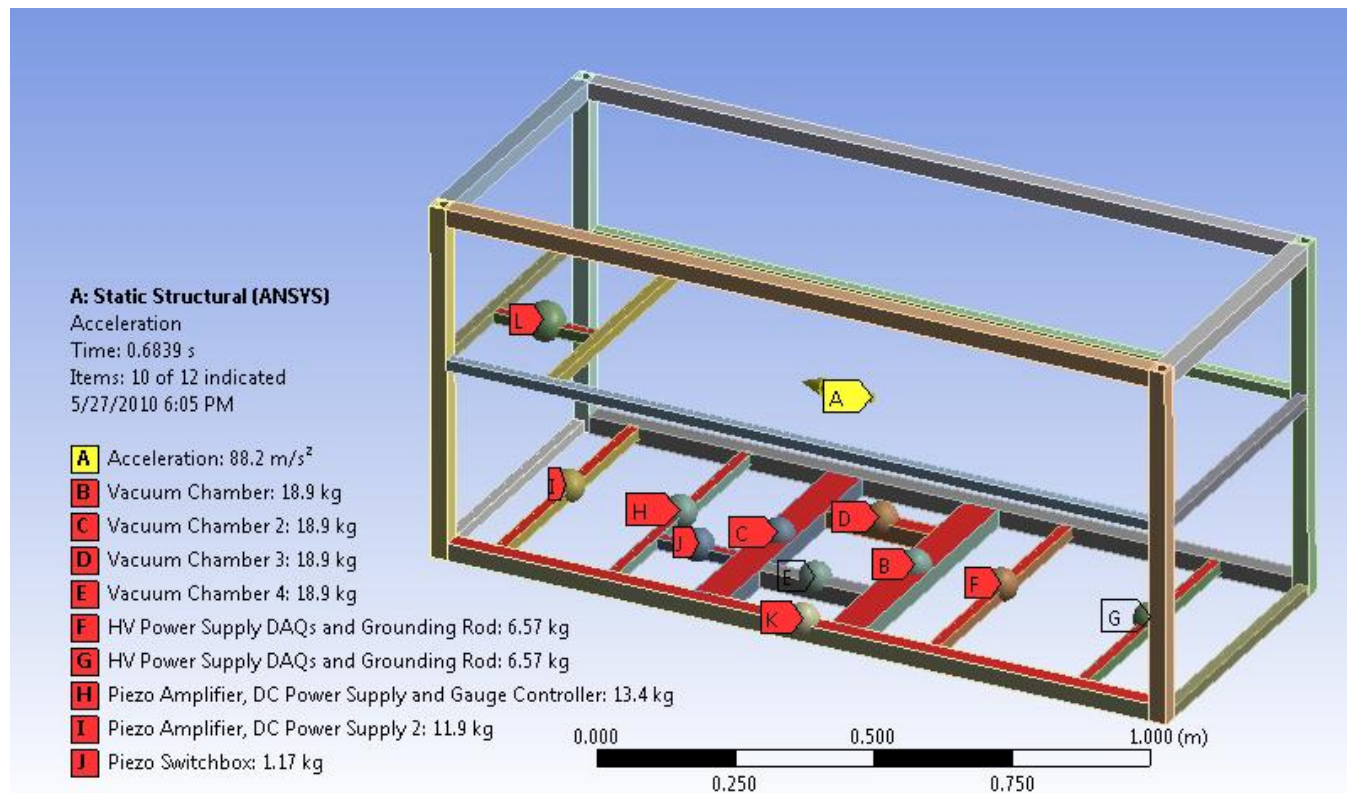


Figure 4: Free body diagram under 9g forward acceleration

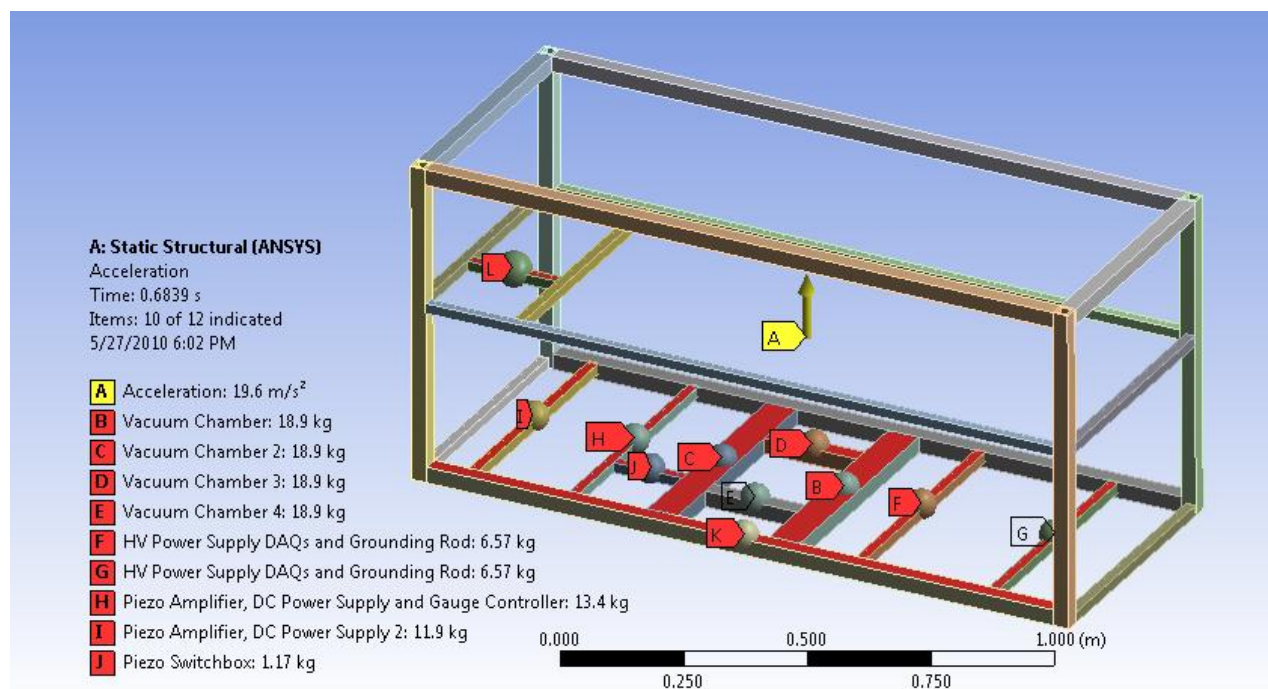


Figure 5: Free body diagram under 2g upward acceleration

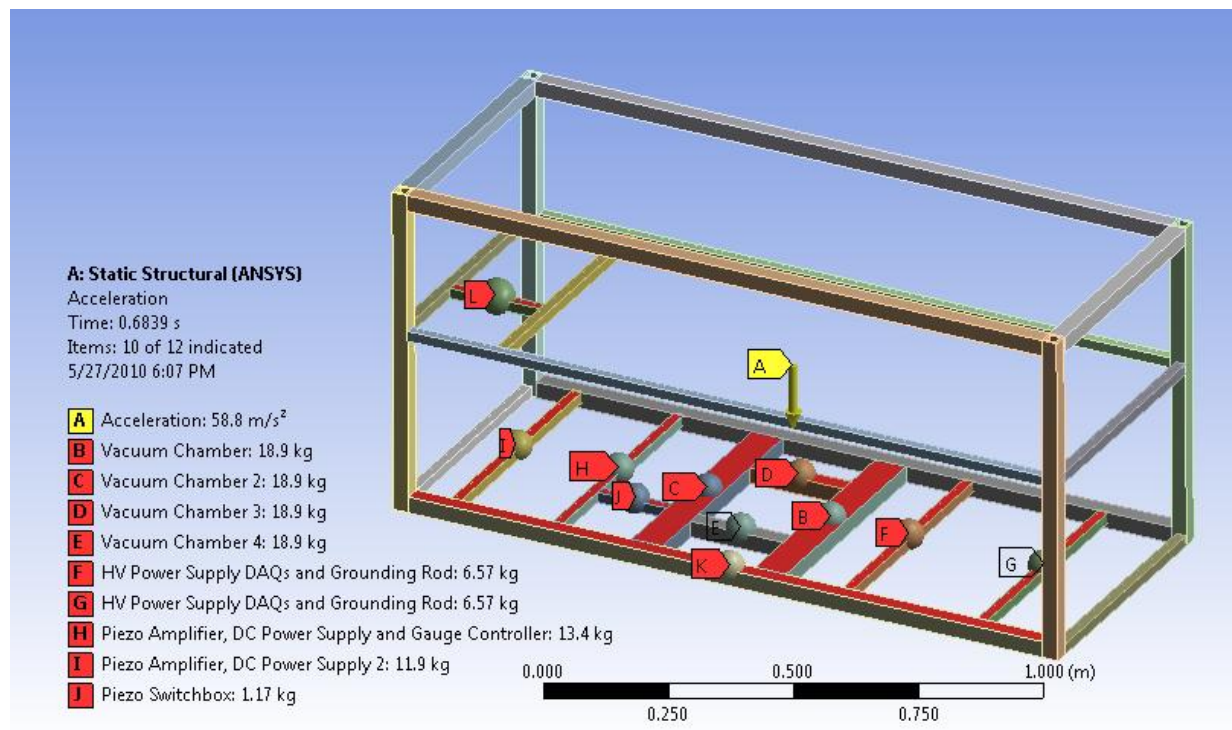


Figure 6: Free body diagram under 6g downward acceleration

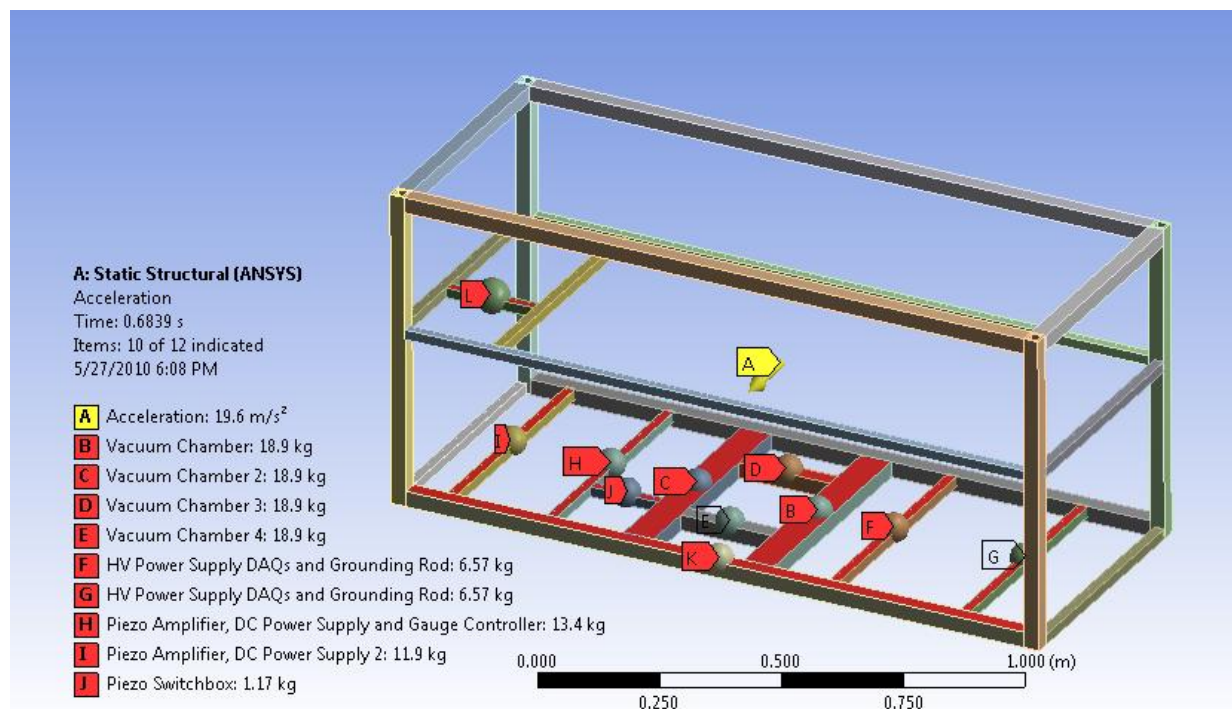


Figure 7: Free body diagram under 2g lateral acceleration

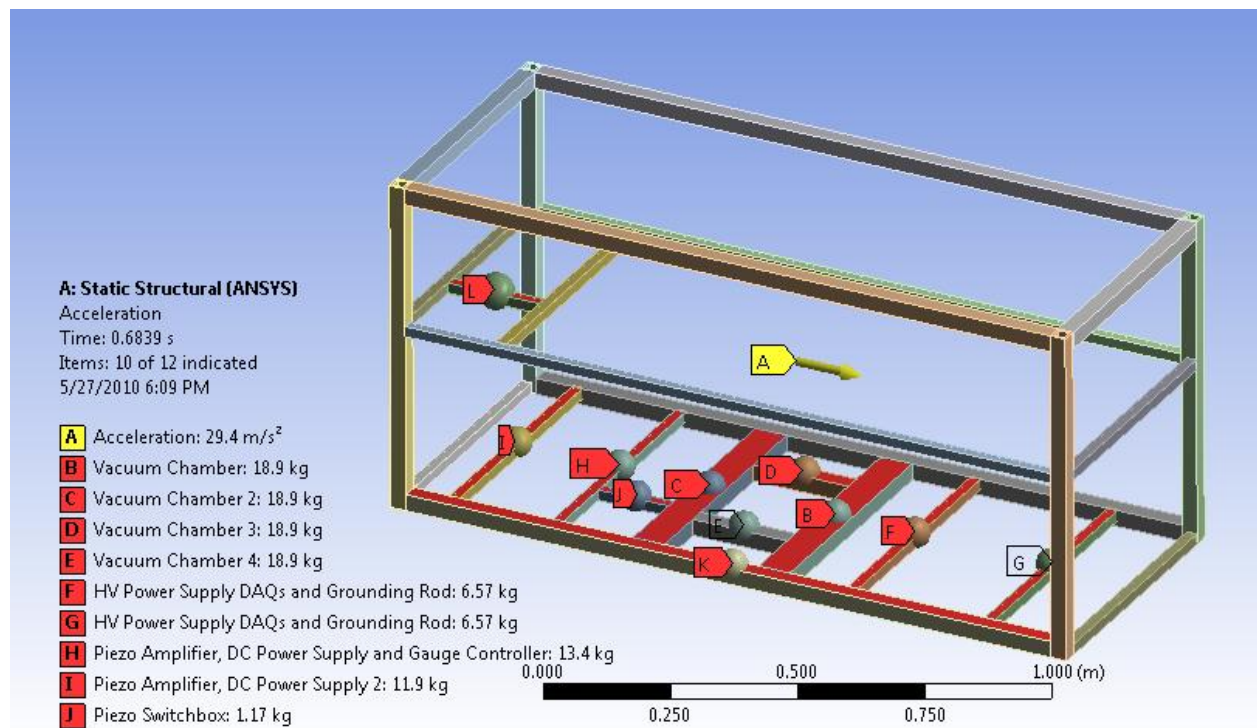


Figure 8: Free body diagram under 3g aft acceleration

The vacuum chamber is rigidly attached to the chassis base using a 3/8" thick, 12" x 14" aluminum plate. The bottom 8" flange is sandwiched between the chamber and base plate, with screws that pass through all three components, fixing them firmly together.

The vacuum base plate experiences a constant weight of approximately 174 lbs due to the vacuum chamber and accompanying parts. The weight was assumed to be distributed over the surface area of the plate, given as 138 in<sup>2</sup>. This pressure force of 8708 Pa was fixed for all loading and the acceleration field varied in magnitude and direction depending on the loading case.

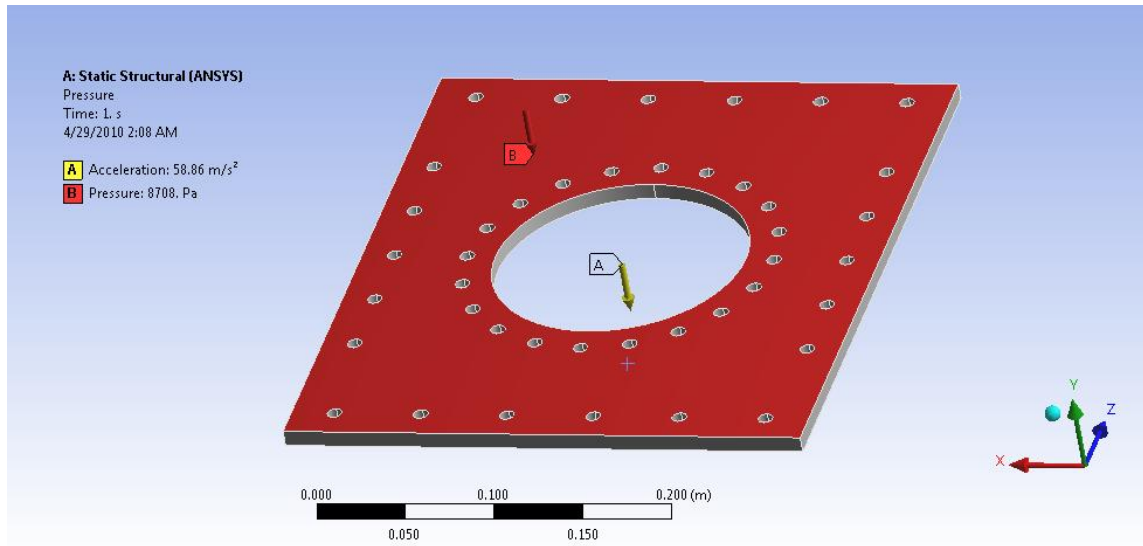


Figure 9: Free body diagram of vacuum mounting plate under 6g downward acceleration

## 7.0 Calculations

### 7.1 Hand Calculations

Key theories and assumptions that simplified all analytical calculations included plane sections remain plane, infinitesimal strain theory, and slender beam theory. This allows the use of linear algebraic systems of equations to solve for moments, stresses, and deformations. Subsequently, the margins of safety and factors of safety were calculated from these analytically obtained stresses. It is also assumed that only the weights of the components under the given accelerations contribute to the stresses of the beams and vacuum support plate.

#### 7.1.1 Cross-Section Dimension Calculations (page 29-30)

Rectangular shell extrusions were used to simplify the actual 80/20 cross-section not only because of their geometric simplicity but because matching the actual area and moment of inertia would involve solving a system of quadratic equations. Square cross-sections were chosen to model the 1010 and 1515-Lite beams while rectangular sections represented the 1530 vacuum support beams. The system of equations for the 2 cross-sections, though both quadratic in form, are slightly different because the rectangular shell involves an additional moment of inertia term. Because of this, the rectangular shell requires solving three equations while the square system is only governed by two equations.

#### 7.1.2 Stress on aircraft mounting bracket (page 35)

Our aircraft mounting brackets have a calculated factor of safety of 3.8 in bending and 41 in shear in the worst case scenario. This is shown in the hand written calculations in the Appendix, section 9.2. The angled aluminum 1.5" x 1.5" brackets span the length of the chassis. These experience both bending and shear forces as described in the appendix. A few sample hand

calculations are included that exhibit their strength in a worst case scenario. Note that the applied forces are halved because we are using two fasteners to the aircraft.

Euler-Bernoulli beam theory is generally used for long and slender beams in which the length of the beam may be more than 30-40 times greater than the dimensions of the cross-section area. Though the portion of the aircraft mounting bracket is a very short beam, Euler-Bernoulli equations still apply because of the static and uniform nature of the loading. This may also be viewed as a limiting case of the more general Timoshenko beam equations which are more suited towards non-uniform and time varying loads and deformations. The maximum stress of this component was 10.5 ksi with a factor of safety of 3.8.

The 9g loading not only produces bending stresses within the vertical component of the mounting bracket but also exerts a shear force on the horizontal component attached to the floor. However, because of its large area, this component is subject to a rather low shear stress. The net shear force was found to be 3513.6 lb. The factor of safety of 41 in this instance is very large and means that shear loading of the aircraft mounting bracket is relatively insignificant.

Thus, our proposed mounting brackets comply with all NASA requirements and have been verified quantitatively. Our added mass will not be a safety concern as our factors of safety rest comfortably above two.

### **7.1.3 Floor Fittings (page 36)**

The 9g loading of the entire chassis exerts forces on the floor of the 727 not to exceed 3000 lbs of force. Our chassis is attached on four corners and weighs 350 lbs with contingency. Calculations were performed at an even worse case scenario of 390 lbs and the floor maintains a factor of safety of 3.4.

### **7.1.3 Loads on Bolts due to Overturning Reaction Forces (page 31-32)**

Overturning moments are significant because of the large reaction forces they induce at the edges of long structures. The overturning force in these analyses is due to the 9g acceleration of the entire chassis and can be modeled as a point force acting a distance  $h$  above the ground, with this  $h$  representing a center of mass. This, along with the gravitational force acting at this same center, creates a torque about one edge of the chassis that must be canceled by the torque caused by the vertical reaction force on the other edge. The bolts connecting the chassis to the aircraft will be subject to this load and the overturning force, though each of the 10 bolts will share the load equally. These bolts are subject to net force of 358.6 lb with a factor of safety of 6.8.

The 12 bolts connecting the vacuum chamber to the chassis will also be subject to overturning forces and their reactions, this time involving the 9g acceleration of the chamber. The overturning force is distributed equally among all 12 bolts while the overturning reaction force is only distributed among the 6 bolts on the right side. The total force acting on the right hand side bolts was found to be 242.8 lb with a factor of safety of 6.5.

#### 7.1.4 Bending, Tension, and Shear due to Overturning Reaction Forces (pages 33-34)

The vacuum chamber mounting plate also exerts a bending force on the 1515-lite beams due to the overturning moment of our chassis. In the worst case 9g loading, the load bearing beams maintain a factor of safety of 11.9, validating the FEA approximation as a concentrated point mass. The beams then, apply forces in tension and in shear to the L-brackets and bolts joining the 1515-Lite beams to the side beams of the chassis. The factor of safety of 8 is well above the limit of 2 specified by NASA.

#### 7.1.5 Beam Calculations

Maximum beam deflections were calculated using equations (1) and (2) for simply supported beams and cantilevers respectively. Vertical beams are assumed to be cantilevers while the upper and middle lateral beams will be modeled as simply supported beams.

$$d = \frac{FL^3}{48EI} \quad (3)$$

$$d = \frac{FL^3}{3EI} \quad (4)$$

where  $d$  is the maximum deflection,  $F$  is the point load,  $L$  is the length of the beam,  $E$  is the elastic modulus, and  $I$  is the moment of inertia. Once again, the pair of equations for maximum stress for simply supported and cantilever are given by

$$\sigma = \frac{FLy}{I} \quad (5)$$

$$\sigma = \frac{FLy}{4I} \quad (6)$$

where  $\sigma$  is the normal stress and  $y$  is the largest distance from the neutral axis to a point on the cross-section. These equations are a considerable overestimation of the actual stresses and deflections in the beam because the elements are actually subject to distributed gravity loads and not point loads. Therefore, if the failure criteria are met for point loads, they will certainly be met for distributed loads.

#### 7.1.6 “Kick Loads” and Impact Analysis

Experimentally, our chassis and surrounding plastic wrap were tested for kickloads of 125 lb over a 2” radius and impact analysis of 180 lbf at 2 ft/s. The experimental components are protected from such impacts on all sides except the front by heavy-duty plastic wrap. It is stretched taut and heated to seal. This was physically confirmed by dropping weights from a height such that the momentum matched an impact of 180 lbf at 2ft/s. Similarly, the kickload was analyzed by applying 125 lb within a two-inch diameter on the plastic.

## 7.2 FEA Analysis

### 7.2.1 Load Application

ANSYS Workbench was chosen to create the mesh and perform analysis on the structure over ANSYS Mechanical APDL, ANSYS ICEMCFD, and Nastran because of its relatively simple mesh generation setup, and its unique global acceleration loading option. Global acceleration loading are an ideal option to have because all the NASA-specified loading conditions the structure must satisfy are acceleration loads. This yields the option of declaring the direction and magnitude the structure will be subjected to and simply superimposing additional point loads and boundary conditions afterwards.

Finally, the thruster mount rod is the only load bearing weld in our setup. However, because the thrusters and probes are contained within the vacuum chamber, the strength of the welded rod does not pose a safety hazard to the flight. The rod is assumed to bear two thrusters and probe units. Should only one thruster be used, the stresses will only decrease. Welding certification papers are included with the TEDP. We have performed a stress analysis to confirm the strength of material. Modal analysis was done through ANSYS WorkBench. However, we also performed FEA on the mounting rod through SimulationExpress in SolidWorks. The rod was clamped where it is welded to the flange and modeled as a cantilever. A distributed force equal to the 9g accelerated weight of probe setup and thrusters was applied to one face of the rod. The results indicated a lowest factor of safety of 3.2 and a yield strength of  $2.07 \times 10^8$  Pa. This was coupled with a max deflection of 780  $\mu\text{m}$ .

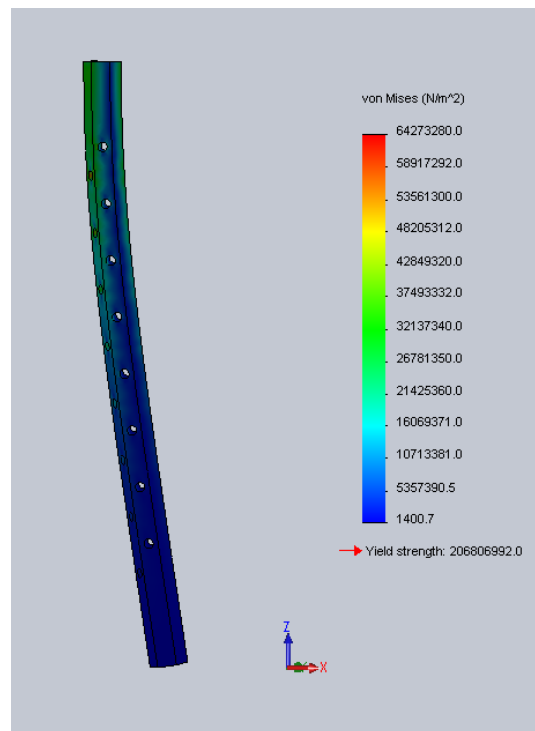


Figure 10: Thruster mount rod shows a maximum yield strength of  $2.07 \times 10^8$  Pa

### **7.2.2 Boundary Conditions and Material Specifications**

All chassis surfaces mounted to the aircraft on the L-bracket are assumed to be fixed with zero deformation. This will mean that the vertical beams will be loaded much like cantilevers, while the upper and middle horizontal beams are assumed to be attached and fixed to whichever beams they are connected to. Though material specifications were all assigned in SolidWorks before importing the model into Workbench, they must be done again in Workbench. Since the Workbench model only consists of the chassis beams, 6061 Aluminum Alloy was selected as the material for all chassis components.

### **7.2.2 Mesh Strategy**

Because of the complexity of the beam cross-sections and Workbench's inability to efficiently compute the mesh of the actual T-Slotted 80/20 geometry, a simplified model was necessary to perform FEA analysis. Thus, a surrogate model was constructed using rectangular shells that matched the given areas and moments of inertias of the actual cross-sections. The equivalent stress values depend on cross-section area and moment of inertia, so it was imperative that our new model matched these two given conditions. Hollow rectangular solids were chosen because of their geometric simplicity with cross-section dimensions chosen to match the area and cross-sections of the actual geometries. Sample calculations are provided in the Appendix section.

This simple geometric approximation and the pointwise loading assumption means that a complex meshing algorithm is not necessary. Fairly accurate results result even from the simplest meshing strategy, Workbench's default rectilinear mesh setup with the largest possible mesh size. This is quite an upgrade over using the actual cross-section of the 80/20 beam, which was far more geometrically complex and was computationally infeasible to generate a mesh

### **7.2.3 Worst Case Scenarios**

Our worst case scenario was found in the 6g downward acceleration. The maximum stresses occurred on the base joints with a maximum equivalent stress of about 109.4 MPa and a factor of safety of 2.2861. The factor of safety is calculated by simply dividing the 80/20 aluminum's yield stress (241 MPa) by the maximum equivalent stress. These point loads also represent a loading configuration worse than the actual setup, in which the masses will exert a distributed load on the beams.

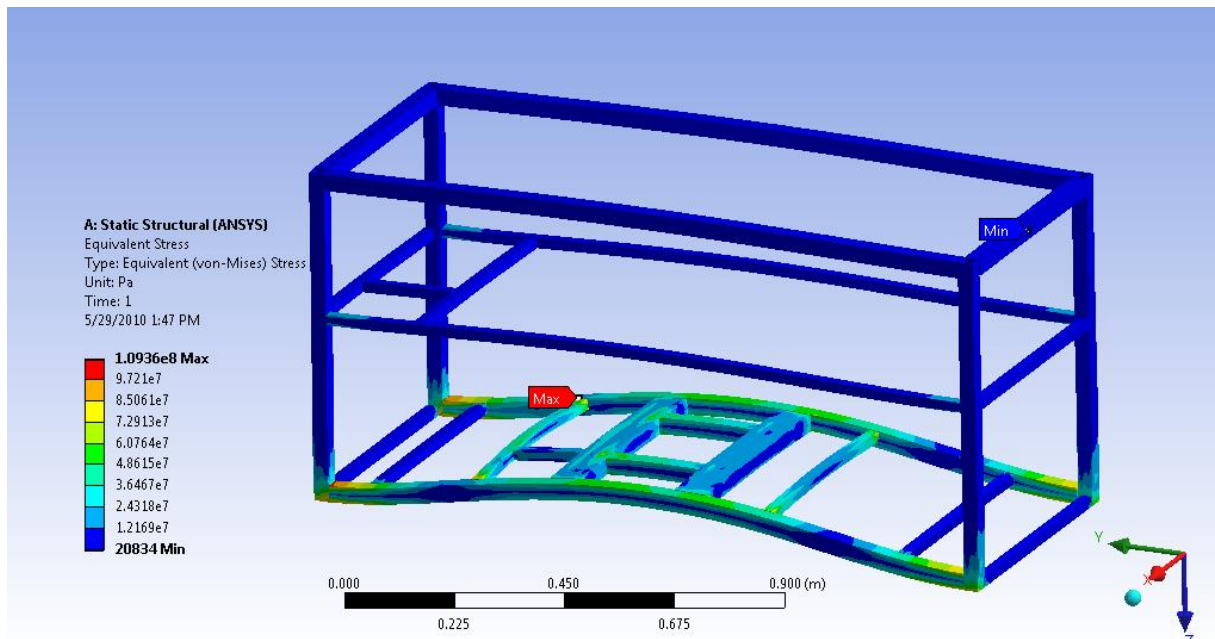


Figure 11: Max stress of 1.0936e8 Pa under 6g downward acceleration

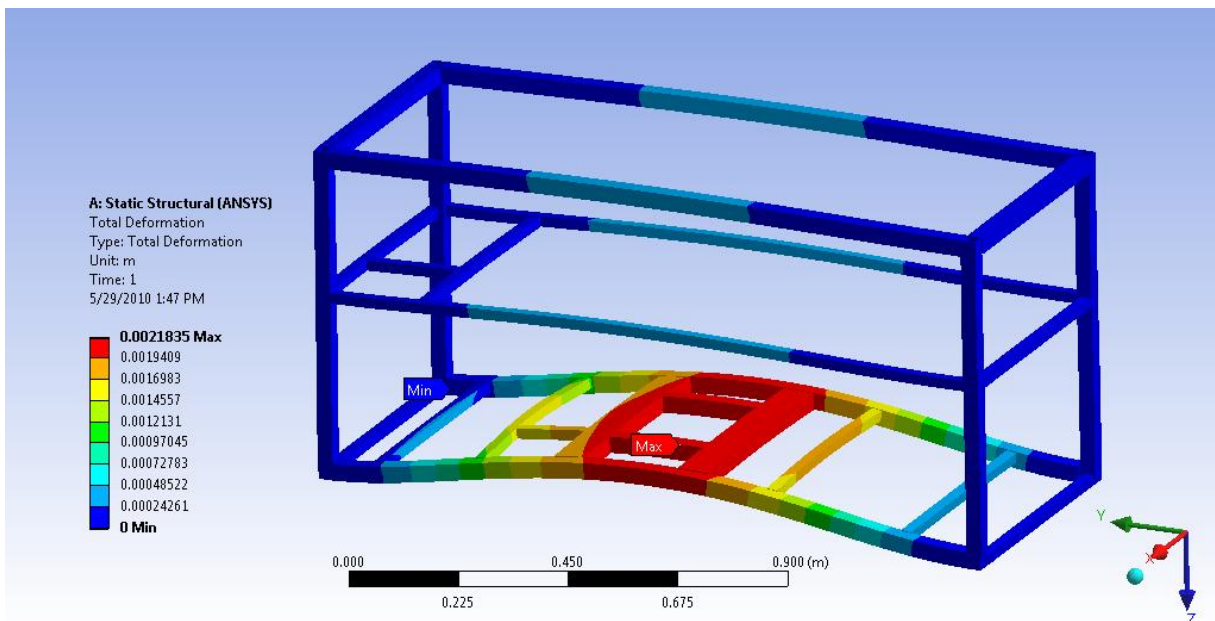


Figure 12: Max deformation of 2.1835e-3 m under 6g downward acceleration

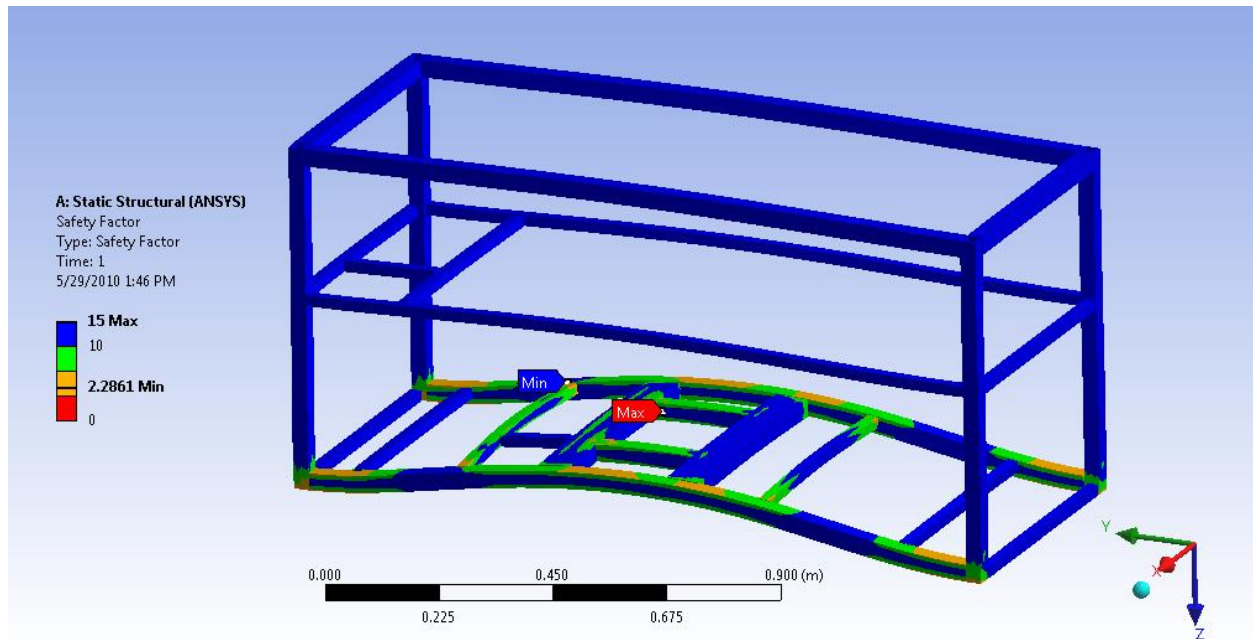


Figure 13: Minimum factor of safety of 2.2861 under 6g downward acceleration

Though the 6g forward acceleration produces the highest stress by a significant margin, we have also included the 9g downward, 2g lateral, 2g up, and 3g aft accelerations in the appendix to quantitatively demonstrate the structural integrity under both of these loading regimes as well. In any event, the lowest factor safety of the very worst case loading configuration has been calculated to be 2.2861, above NASA's required minimum factor of safety of 2.

#### 7.2.4 Scroll Pump Contingency

Because the gate valve can maintain pressure after pumping, it will not be necessary to fly the dry scroll pump with us during flight. However, should the gate valve not function as expected, we may be forced to add the 20.6 lb scroll pump to our chassis. The DC power supply will be replaced by the scroll pump and moved on top of the HV power supply. In this worst case scenario of 9g, our chassis still responds with a factor of safety of 2.0604.

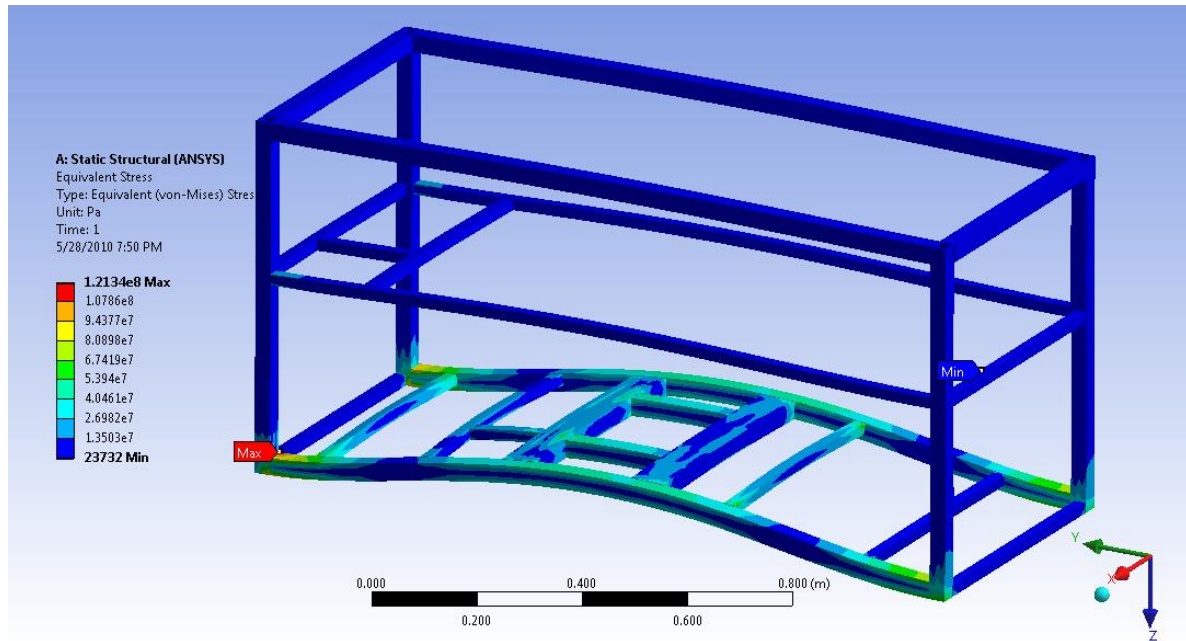


Figure 14: Max stress of 1.2134e8 Pa under 9g forward acceleration

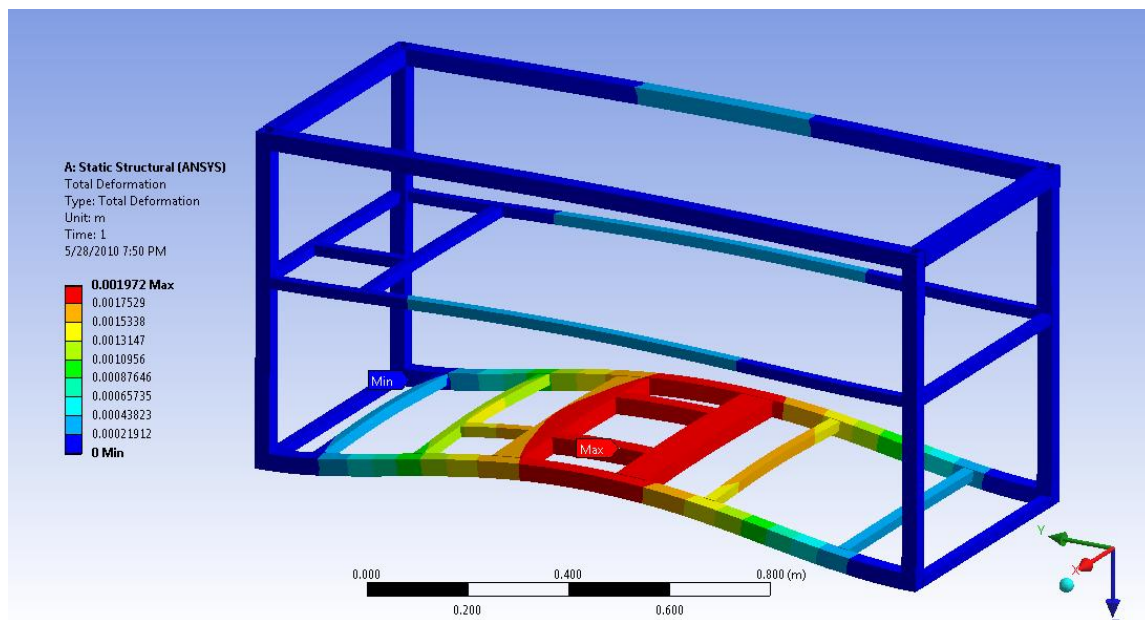


Figure 15. Max deformation of 1.972e-3 m under 9g forward acceleration

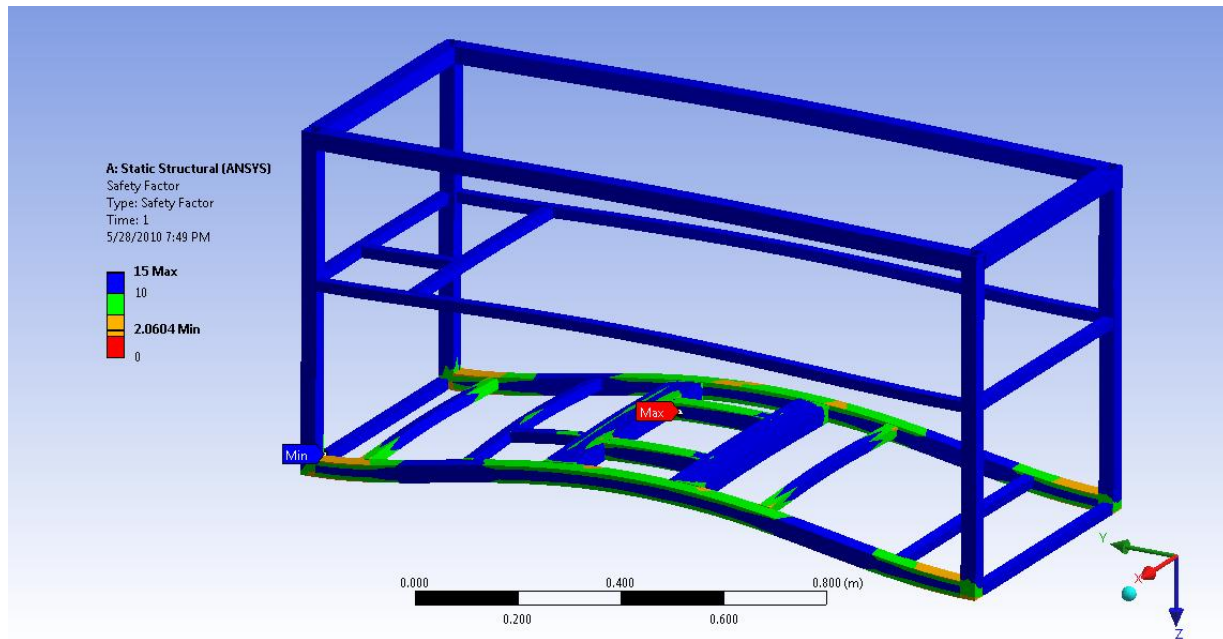


Figure 16. Minimum factor of safety of 2.0604 under 9g forward acceleration

### 7.3 Modal Analysis

Modal and vibration analysis tests were also conducted on the thruster mount because even micrometer scale misalignments of the thruster and probe can profoundly alter test data. Determining the different mode shapes under a range of natural frequencies was the most important task because of the large deformations incurred near these frequencies. Because of the complex geometry of the mount, natural frequencies and prediction of the kinematic response at these conditions were computed using Workbench. Only the first few modes were computed to give a good estimate of how the deformation changes across different natural frequencies. The first 4 modes we obtained from Workbench were 96.2, 99.9, 592.7, and 619.0 Hz.

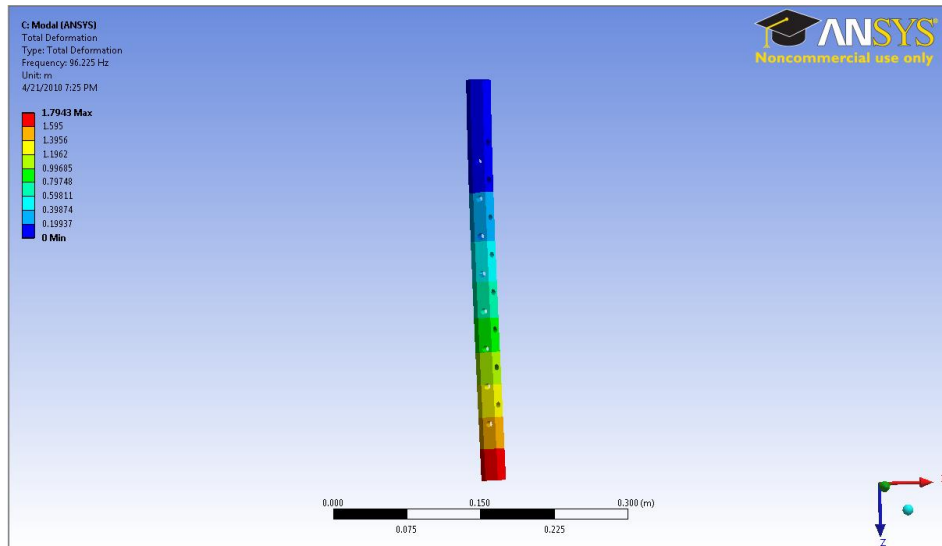


Figure 17. Frequency mode 1 = 96.225 Hz

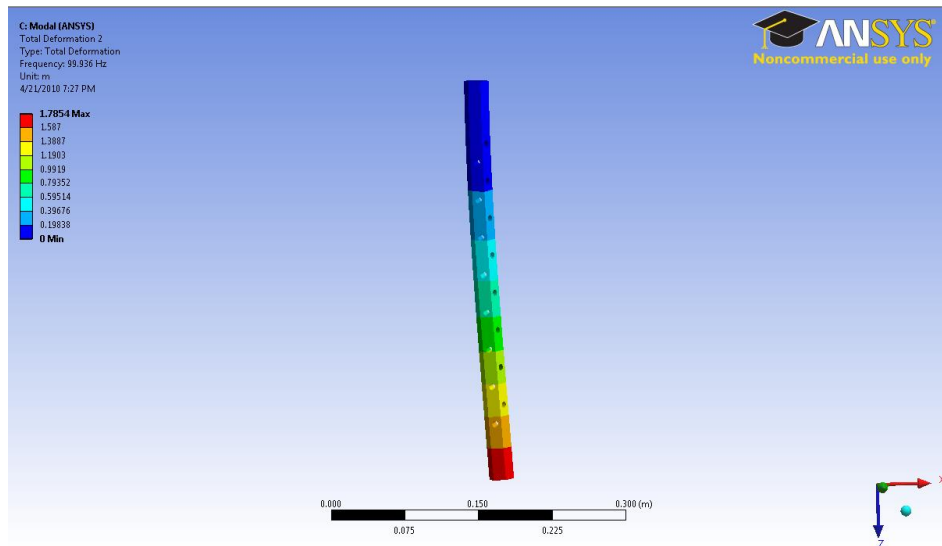


Figure 18. Frequency mode 2 = 99.936 Hz

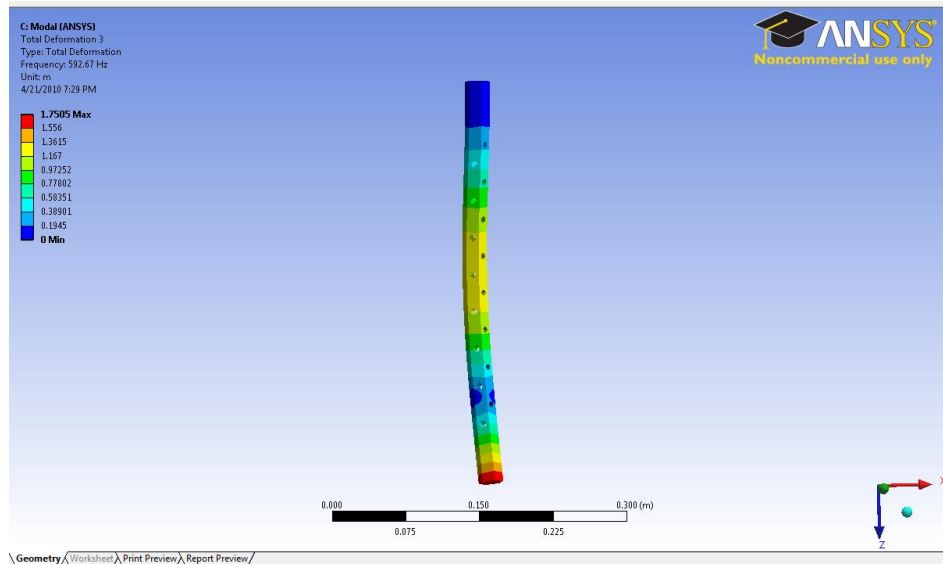


Figure 19. Frequency mode 3 = 592.67 Hz

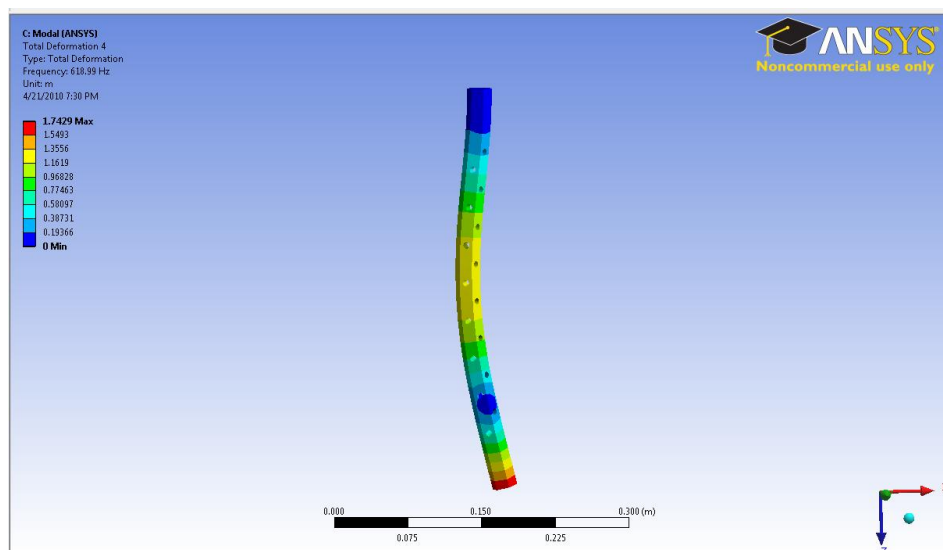


Figure 20. Frequency mode 4 = 618.99 Hz

## 8.0 References

1. *Preparation of Stress Analysis Reports*, JSC, NASA Johnson Space Center, 2009
2. *Metallic Materials Properties Development and Standardization (MMPDS-04)*. 2009 Battelle Memorial Institute.  
[http://knovel.com/web/portal/browse/display?\\_EXT\\_KNOVEL\\_DISPLAY\\_bookid=2186&VerticalID=0](http://knovel.com/web/portal/browse/display?_EXT_KNOVEL_DISPLAY_bookid=2186&VerticalID=0)

## 9.0 Appendices

### 9.1 Mass Budget

Item	Quantity	Unit Weight (lbs)	Contingency	Mass with Contingency
Chassis - 80/20 + Bolts +				
Hardware	1	73.5	5%	77.2
Chassis - Chamber Mounting Plate	1	5.4	5%	5.7
Chassis - Plastic Wrap	1	0.6	5%	0.6
Grounding Rod	1	1.5	5%	1.6
HV Power Supply	1	21.6	5%	22.7
NI USB-6218 DAQ	1	0.6	5%	0.6
NI USB-6255 DAQ	1	2.7	5%	2.8
DAQ box	1	1.3	15%	1.5
Panasonic Toughbook	1	9.0	5%	9.5
Piezoelectric Amplifier	1	25.6	5%	26.9
Piezo Switch Box	1	2.5	5%	2.6
Wiring	1	10.0	15%	11.5
Probe Setup	1	1.0	20%	1.2
Shielding Mesh	1	2.0	15%	2.3
DC Power Supply	1	24.8	5%	26.0
Thruster	1	2.0	15%	2.4
Vacuum System - BNC				
Feedthrough	1	0.6	5%	0.6
Vacuum System - 8" Viewport	2	5.3	5%	11.1
Vacuum System - Chamber	1	51.5	5%	54.1
Vacuum System - Chamber Bolts	1	11.1	10%	12.2
Vacuum System - Converter				
Flange 6" to 2.75"	1	5.3	5%	5.6
Vacuum System - Converter				
Flange 6" to 1.33"	1	6.0	15%	6.9
Vacuum System - Gaskets	15	0.1	10%	2.1
Vacuum System - Mounting rod				
and 8" flange	1	15.2	5%	16.0
Vacuum System - 8" D-Sub	1	12.0	5%	12.6
Vacuum System - Leak Valve	1	2.6	5%	2.7
Vacuum System - Pressure gauge				
Controller	1	2.5	20%	3.0
Vacuum System - Pressure Gauge	1	1.6	5%	1.7
Vacuum System - Gate Valve	1	12.0	5%	12.6
Vacuum System - HV	2	1.4	5%	2.9

Feedthrough				
Vacuum System - Pressure Burst				
Valve	1	0.3	5%	0.4
Vacuum System - HV Caps	2	0.3	10%	0.6
Systems Margin	1	10.0	0%	10.0
		<b>Expected</b>		
		<b>Weight</b>		<b>w/Contingency</b>
<b>Total (lbs.)</b>		330.3		350.2

## 9.2 Hand Calculations

Prepared By: David Yu	Zero-g ElectroStatic Thruster Testbed Reflight	Page No.
Checked By:		Report No.
Date 4/28/10	Title Area and Moment of Inertia Match 1515-Lite	Model No.
Ref.		CWG No. -

80/20 Beam - Given actual area ( $A_a$ ) and inertia ( $I_a$ )

Goal: Assuming Cross-section Geometry is a concentric rectangular shell, Find dimensions such that a and b such that shell area and inertia match actual values.

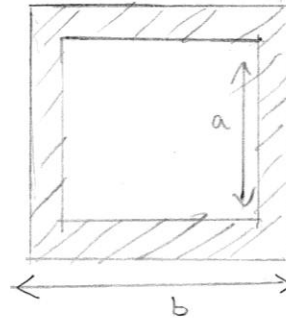
Example: 1515-Lite

Given 1)  $A_a = 1.15 \text{ in}^2$

Given 2)  $I_a = 0.26 \text{ in}^4$

$$\text{Eq. 1) } - A_a = b^2 - a^2$$

$$\text{Eq. 2) } I_a = \frac{b^4 - a^4}{12}$$



Factoring Eq. 2

2 Unknowns a, b

and Plugging Eq. 1 in with 2 equations.

$$\text{Eq. 2 Becomes } 12I_a = (b^2 - a^2)(b^2 + a^2)$$

$$\rightarrow 12I_a = A_a(b^2 + a^2)$$

$$\text{Rewrite Eq. 1 and Eq. 2 as } \rightarrow \frac{12I_a}{A_a} = b^2 + a^2$$

$$\text{Eq. 1) } - A_a = b^2 - a^2$$

$$\text{Eq. 2) } - \frac{12I_a}{A_a} = b^2 + a^2$$

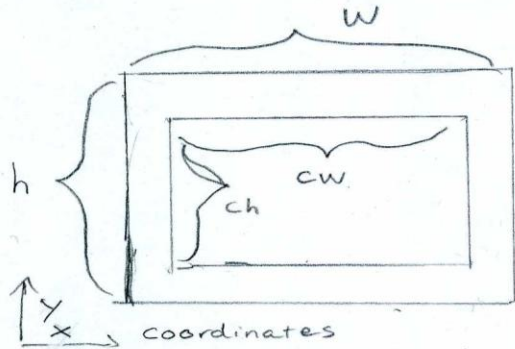
$$\rightarrow \sqrt{\frac{A_a + \frac{12I_a}{A_a}}{2}} = b$$

$$\text{Thus } b = 1.39 \text{ in}$$

$$a = 0.88 \text{ in}$$

and

$$\sqrt{\frac{\frac{12I_a}{A_a} - A_a}{2}} = a$$

Prepared By: David Yu	Zero-g ElectroStatic Thruster Testbed Reflight	Page No.
Checked By:		Report No.
Date 4/28/10	Title Area and Moment of Inertia Match 1530	Model No. CWG No.
Ref.	<p>Unknown variables height h width w Scaling Factor c</p>  <p>Given <math>A, I_{xx}, I_{yy}</math></p> <p>Eq. 1) - <math>A = wh - c^2wh = wh(1 - c^2)</math></p> <p>Eq. 2) - <math>I_{xx} = \frac{wh^3 - c^4wh^3}{12}</math></p> <p>Eq. 3) - <math>I_{yy} = \frac{hw^3 - c^4hw^3}{12}</math></p> <p>Substituting Eq. 1 into Eq. 2 and Eq. 3 Yields New Equations</p> <p>A) <math>A = wh(1 - c^2)</math></p> <p>B) <math>I_{xx} = \frac{A}{12} (1 + c^2) h^2</math></p> <p>C) <math>I_{yy} = \frac{A}{12} (1 + c^2) w^2</math></p> <p>Solving these yields</p> <div style="border: 1px solid black; padding: 5px; width: fit-content;"> <p><math>h = 1.4 \text{ in}</math>  <math>w = 2.7 \text{ in}</math>  <math>c = 0.67</math></p> </div> <p>3 equations 3 unknowns</p> <p><b>Given</b>  <math>A = 2.09 \text{ in}^4</math>  <math>I_{xx} = 0.49</math>  <math>I_{yy} = 1.82</math></p>	

Prepared By: David Yu	Zero-g ElectroStatic Thruster Testbed Reflight	Page No. 28-49
Checked By:		Report No.
Date 4/28/10	Title Bolts Overturning Stress	Model No.
Ref.		CWG No.

$\sigma_y = 32 \text{ ksi}$   
 $d = 0.3125 \text{ in}$   
Eq. 1)  $F_{allow} = \frac{\pi d^2 \sigma_y}{4}$   
 $\rightarrow F_{allow} = 2454.4 \text{ lbf}$

Moment Balance  
Eq. 2) About A

$\Sigma M_A = 0 =$   
 $W_{tot} \frac{L}{2} + F_{MAX} h - PL$

Eq. 3)  $F_{MAX} = 9 W_{TOT}$

Eq. 4)  $P = \frac{W_{tot}}{2} + \frac{F_{MAX} h}{L}$

$\Rightarrow P = W_{TOT} \left( \frac{1}{2} + \frac{9h}{L} \right)$

$W_{TOT} = 390.4 \text{ lb}$   
 $h = 8.75''$   
 $L = 59''$

$P = 390.4 \left( \frac{1}{2} + \frac{9(8.75)}{59} \right) = 716.3 \text{ lbs}$   
 $T = F_{MAX}$

Eq. 5)  $F = \sqrt{T^2 + P^2}$   
 $F = \sqrt{3513.6^2 + 716.3^2} = 3585.9 \text{ lb}$

$F_{bolt}$  (Force on each bolt)  $N = 10 \text{ bolts}$

$F_{bolt} = \frac{F}{N} = 358.6 \text{ lb}$

$F.O.S = \frac{F_{allow}}{F_{bot}} = 6.8$

M.O.S = F.O.S - 1 = 5.8

Prepared By: David Yu	Zero-g ElectroStatic Thruster Testbed Reflight	Page No. 29/5
Checked By:		Report No.
Date 4/28/10	Title Chamber Support Bolts	Model No.
Ref.		CWG No.

$W_c$  (Weight of Chamber)  
 $F_{cham}$  (Force on Chamber)

Eq. 1) Total Moment About A = 0

$$\sum M_A = 0 = F_{cham} h + \frac{W_c L_c}{2} - P_c L_c$$

6 bolts on left side of plate  
 and 6 bolts on right side of plate.

From Eq. 1  $\Rightarrow P_c = \frac{W_c}{2} + \frac{F_{cham} h}{L_c}$

Using  $L_c = 12 \text{ in}$   
 $W_c = 174 \text{ lb}$   
 $h = 8.75 \text{ in}$

$F_{cham} = 9 W_c$   
 $P_c = W_c \left( \frac{1}{2} + \frac{9h}{L_c} \right)$   
 $P_c = 1228.9 \text{ lb}$

Stress per Bolt

Horizontal Stress per Bolt  $\Rightarrow F_{x \text{ bolt}} = \frac{F_{cham}}{12}$  (Act on all 12)  
 Vertical Stress per Bolt  $\Rightarrow F_{y \text{ bolt}} = \frac{P_c}{6}$  (Act on only on right half)

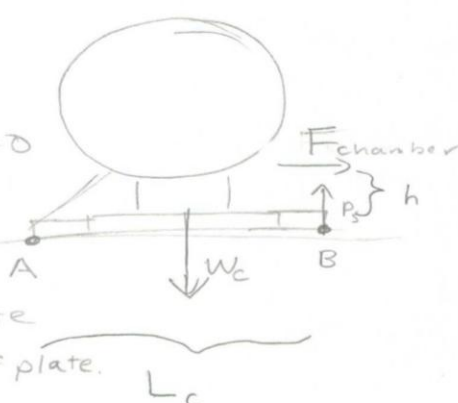
$F_{x \text{ bolt}} = \frac{9 W_c}{12} = 130.5 \text{ lb}$   
 $F_{y \text{ bolt}} = \frac{P_c}{6} = 204.8 \text{ lb}$

$F_{\text{bolt}} = \sqrt{F_{x \text{ bolt}}^2 + F_{y \text{ bolt}}^2} = 242.8 \text{ lb}$

Allowable Force  $d = \frac{1}{4} \text{ in}$   $\sigma_{yield} = 32 \text{ ksi}$

Eq. 2)  $F_{allow} = \sigma_{yield} \left( \pi \left( \frac{d}{2} \right)^2 \right) = 1570.8 \text{ lbs}$

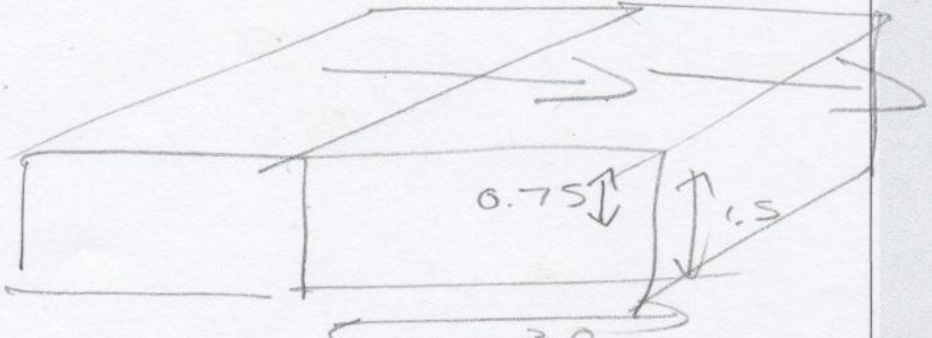
$F.O.S_{\text{bolt}} = \frac{F_{allow}}{F_{\text{bolt}}} = \frac{1570.8}{242.8} = 6.5$   
 $M.O.S = F.O.S - 1 = 5.5$



Prepared By: <i>David Yu</i>	Zero-g ElectroStatic Thruster Testbed Reflight	Page No.
Checked By:		Report No.
Date <i>5/29/10</i>	Title <i>1515 Bending</i>	Model No.
Ref.		CWG No.

Due to Vacuum Chamber,  $9g$



$M = (87)(9)(10.5)$   
 $= 8221.5$

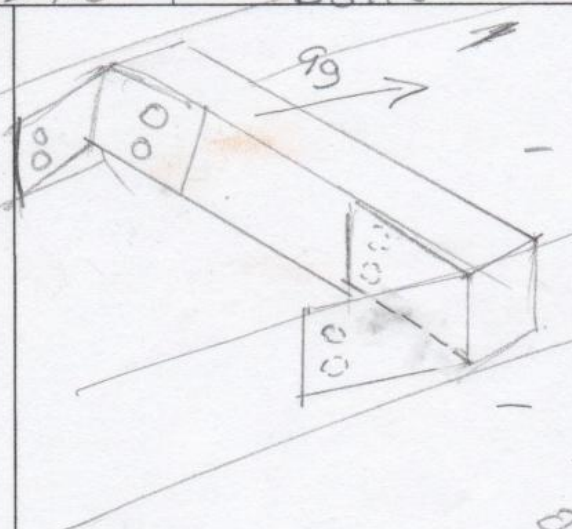
$\sigma_{yy} = \frac{M y}{I}$

$\sigma_{yy} = \frac{(8221.5)(0.75)}{2.3}$   
 $= 2681.9 \text{ ksi}$

$I = 2.3 \text{ in}^4$

$\sigma_{\text{yield}} = 32 \text{ ksi}$

$F.S. = \frac{32 \text{ ksi}}{2.681 \text{ ksi}}$   
 $= 11.9$

Prepared By: <i>David Yu</i>	Zero-g ElectroStatic Thruster Testbed Reflight	Page No.
Checked By:		Report No.
Date <i>5/29/10</i>	Title <i>Support/Side Beam Bolts</i>	Model No. CWG No.
Ref.	 <p> 2 Beams  - 4 Bolts Per Beam in Tension  - 4 Bolts Per Beam in Shear  - 8 Bolts Total in Tension and 8 Bolts in Shear </p> $F_{allow} = \sigma_{yield} (\pi) \left(\frac{1}{8}\right)^2 = 1570.8$ $F_{bolt} = \frac{(17416)(9)}{8} = 19616$ <div style="border: 1px solid black; padding: 10px; width: fit-content; margin: 10px auto;"> <math display="block">F.O. = \frac{1570.8}{196} = 8</math> </div>	

Prepared By: David Yu	Zero-g ElectroStatic Thruster Testbed Reflight	Page No. 30 45
Checked By:		Report No.
Date 4/28/10	Title Stresses on Aircraft Mounting Bracket.	Model No.
Ref.		CWG No.

Eq. 1)  $F_{MAX} = 9W_{TOT}$   
 $F_{MAX} = 3513.6 \text{ lb}$

Eq. 2 - Using Bernoulli-Euler Beam Theory.

$$\sigma_{\text{bend}} = \frac{My}{I}$$

$$M = \frac{F_{MAX} b}{2} = \frac{2635.2 \text{ lb}}{2}, y = \frac{t}{2} = 0.125''$$

$$I = \frac{L t^3}{12} = \frac{1}{32}$$

$$\sigma_{\text{bend}} = \frac{(2635.2)(0.125)}{\frac{1}{32}} = 10.5 \text{ ksi}$$

Eq. 4  $F.O.S._{\text{bend}} = \frac{\sigma_{\text{yield}}}{\sigma_{\text{bend}}} = \frac{40}{10.5} = 3.8$

$F.O.S._{\text{bend}} = 3.8$

Force Allowable for Shear  $F_y$

Eq. 5  $F_y = \sigma_{\text{yield}} A = \sigma_{\text{yield}} b L = (40 \text{ ksi})(1.5'')(24'')$   
 $\rightarrow F_y = 144 \times 10^3 \text{ lb}$

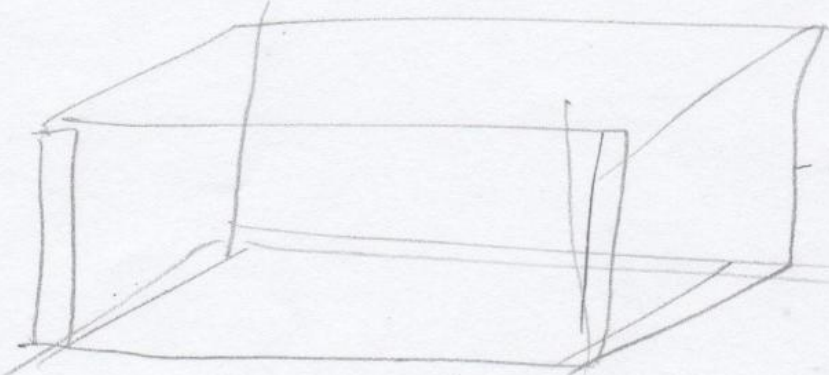
$F_{\text{shear}} = F_{MAX} = 3513.6 \text{ lb}$

$$F.O.S._{\text{(shear)}} = \frac{F_y}{F_{\text{shear}}} = 41$$

M.O.S. = F.O.S. - 1 = 40

Prepared By: <i>David Yu</i>	Zero-g ElectroStatic Thruster Testbed Reflight	Page No.
Checked By:		Report No.
Date <i>5/29/10</i>	Title <i>Floor Stresses</i>	Model No.
Ref.		CWG No.

*A*      *9g Force*



Assume *9g* Force of  
Chassis evenly Distributed  
On 4 Bottom Beams

$$F_{net} = (39016)(9) = 351016$$

$$F_{allow} = 30000 \text{ lb}$$

$$F.S. = \frac{F_{allow}}{F_{net}} = 3.4$$

## Hand Calculated Chassis Beam Stresses and Deflections

	Beam Weight	Applied Load (N)	Applied Load (lbs)	Total Load (1 g)	Stresses from beam weight (MPa)	Stress in 6g Down (MPa)	Stress in 9g Forward (MPa)	Stresses in 2g up (MPa)	Stresses in 2 g Lateral (MPa)	Max Deflection (µm)
1010 (56 in) Top Front	2.42	0.00	0.00	2.42	2.92	17.51	26.42	6.53	9.23	50.60
1010 (56 in) Top Back	2.42	0.00	0.00	2.42	2.92	17.51	26.42	6.53	9.23	50.60
1010 (21 in) Top Left	0.94	0.00	0.00	0.94	0.43	2.56	3.86	0.95	1.35	1.04
1010 (21 in) Top Right	0.94	0.00	0.00	0.94	0.43	2.56	3.86	0.95	1.35	1.04
1010 (56 in) Middle Front	2.42	0.00	0.00	2.42	2.92	17.51	26.42	6.53	9.23	50.60
1010 (56 in) Middle Back	2.42	0.00	0.00	2.42	2.92	17.51	26.42	6.53	9.23	50.60
1010 (21 in) Middle Right	0.94	0.00	0.00	0.94	0.43	2.56	3.86	0.95	1.35	1.04
1010 (21 in) Middle Left	0.94	0.00	0.00	0.94	0.43	2.56	3.86	0.95	1.35	1.04
1010 (21 in) Bottom Right	0.94	50.11	11.35	12.29	0.43	33.35	6.75	5.62	5.70	1.04
1010 (21 in) Bottom Left	0.94	158.70	35.95	36.89	0.43	100.10	37.09	16.71	16.73	1.04
1010 (21 in) Bottom	0.94	50.02	11.33	12.27	0.43	33.35	6.75	5.62	5.70	1.04
1010 (21 in) Bottom	0.94	158.70	35.95	36.89	0.43	100.10	37.09	16.71	16.73	1.04
1515 (56 in) Bottom Front	4.87	4.41	1.00	5.87	1.34	9.71	13.41	3.13	4.33	156.69
1515 (56 in) Bottom Back	4.87	22.95	5.20	10.07	1.34	16.65	15.71	3.86	4.88	156.69
1515 (21 in) Bottom Left	2.43	0.00	0.00	2.43	1.10	1.51	9.90	2.21	3.31	4.12
1515 (21 in) Bottom Right	2.43	0.00	0.00	2.43	1.10	1.51	9.90	2.21	3.31	4.12
1515 (28 in) Vertical Beam	2.53	0.00	0.00	2.53	0.35	2.09	3.17	0.78	1.11	10.18
1515 (28 in) Vertical Beam	2.53	0.00	0.00	2.53	0.35	2.09	3.17	0.78	1.11	10.18
1515 (28 in) Vertical Beam	2.53	0.00	0.00	2.53	0.35	2.09	3.17	0.78	1.11	10.18
1515 (28 in) Vertical Beam	2.53	0.00	0.00	2.53	0.35	2.09	3.17	0.78	1.11	10.18
1530 (21 in) Bottom Left	5.01	205.00	46.44	51.45	0.28	17.10	3.79	2.90	2.97	4.51

1530 (21 in) Bottom Right	5.01	205.00	46.44	51.45	0.28	17.10	3.79	2.90	2.97	4.51
1515 (21 in) Bottom Front	4.87	205.00	46.44	51.31	0.50	31.82	6.97	5.40	5.51	8.26
1515 (21 in) Bottom Back	4.87	205.00	46.44	51.31	0.50	31.82	6.97	5.40	5.51	8.26
1010 (21 in) Middle Inside C	0.94	21.00	4.76	5.70	0.43	15.46	4.62	2.71	2.88	1.04
1010 (21 in) Middle Inside C	0.94	21.00	4.76	5.70	0.43	15.46	4.62	2.71	2.88	1.04
1010 (21 in) Middle Support	0.94	47.70	10.81	11.75	0.43	31.87	6.55	5.38	5.46	1.04
1010 (21 in) Bottom Support	0.94	10.59	2.40	3.34	0.43	9.07	4.12	1.74	1.98	1.04

Section 7.1 details how the stresses were derived.

The beam weight is due to the mass of the beam itself while the applied load corresponds to the total weight of components acting on the beam as shown in the free body diagrams in section 6.0.

## 9.2 Chassis Stresses, Deflections, and Factors of Safety Under All Accelerations

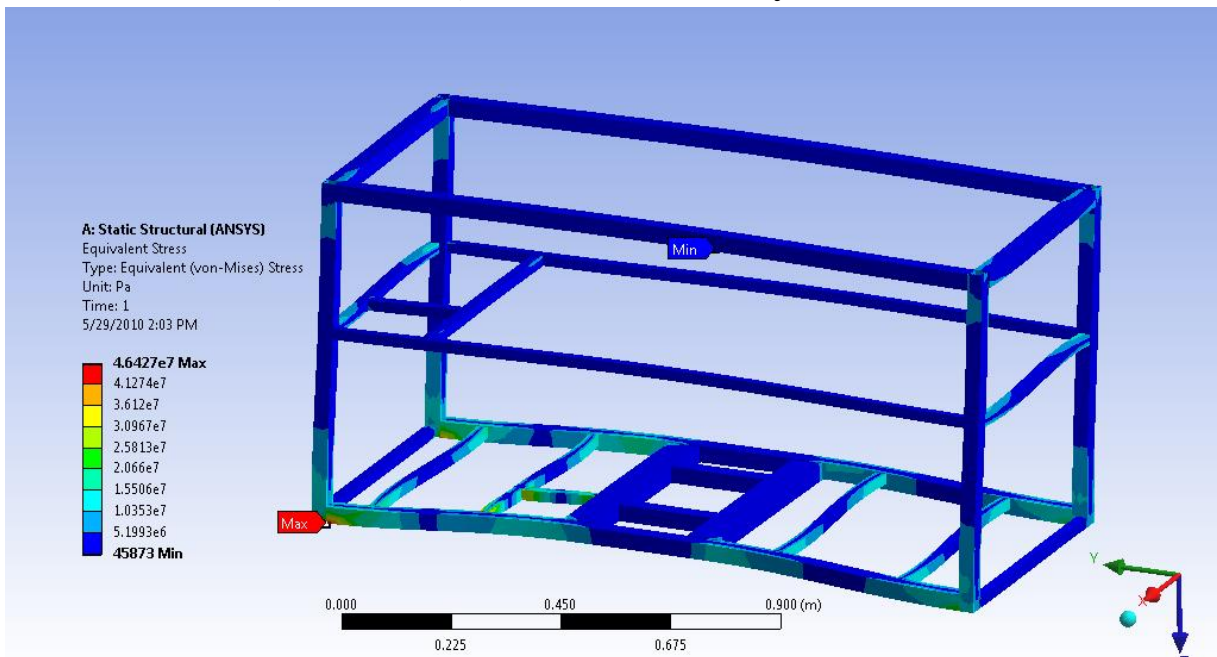


Figure 21: Max stress of 4.6427e7 Pa under 2g lateral acceleration

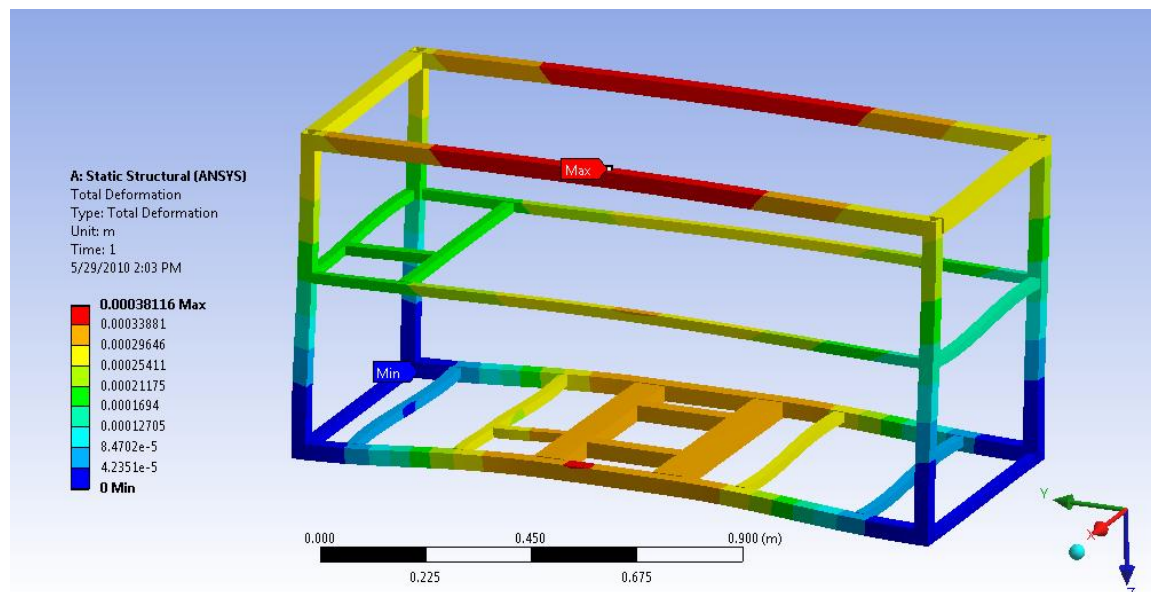


Figure 22: Max deformation of 3.8116e-4 m under 2g lateral acceleration

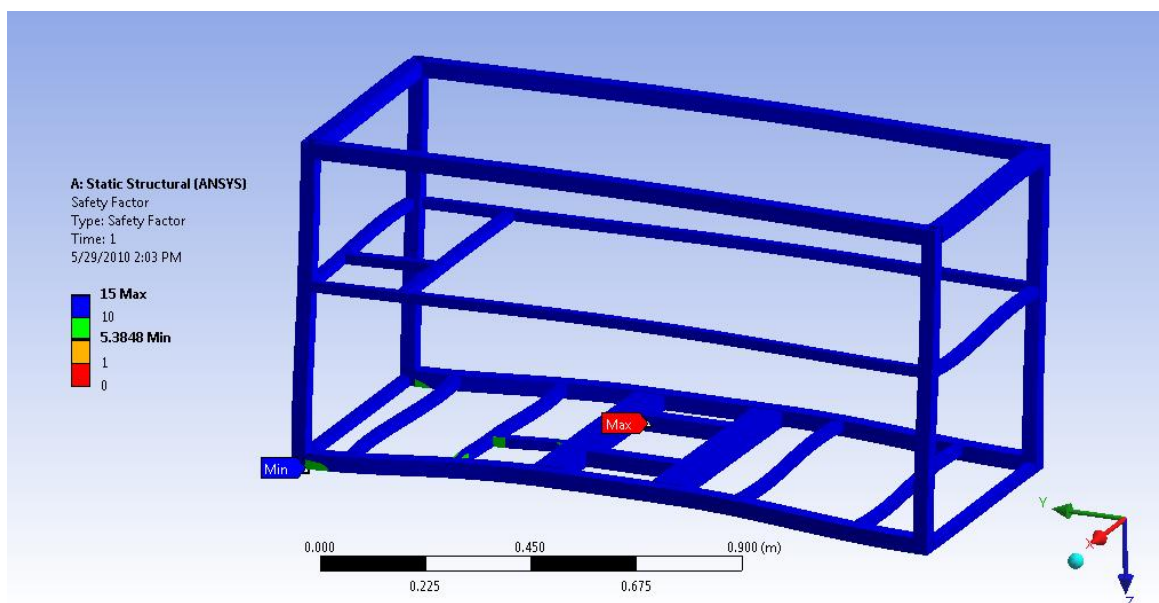


Figure 23: Minimum factor of safety of 5.3848 under 2g lateral acceleration

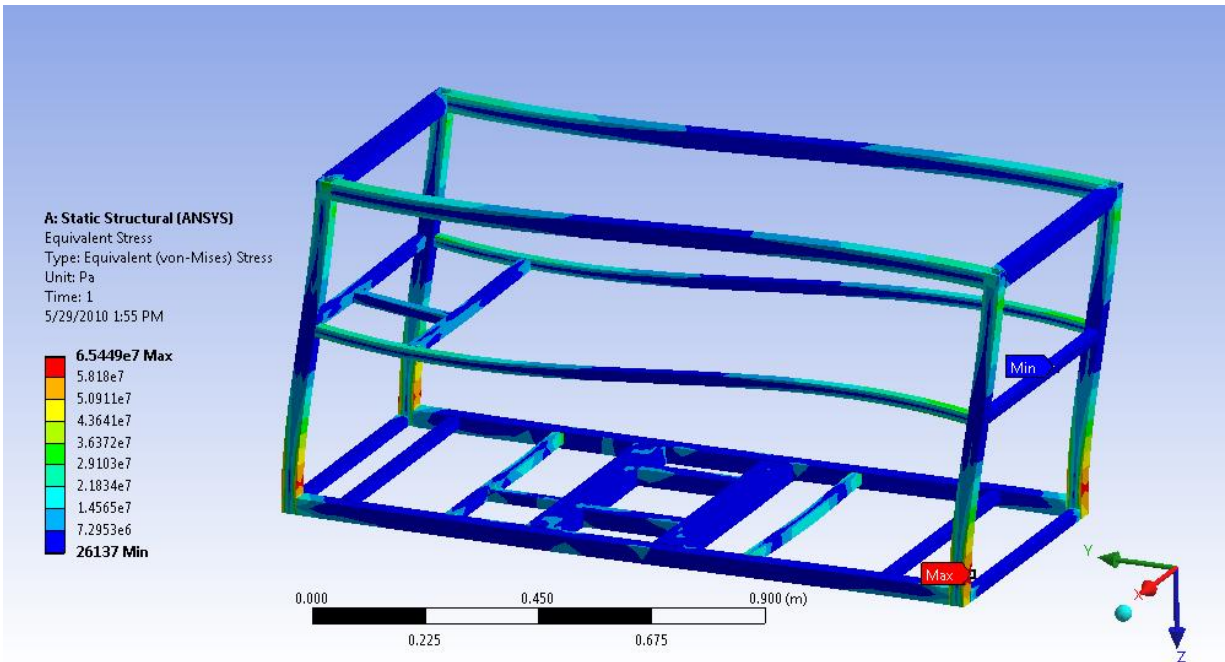


Figure 24: Max stress of 6.5449e7 Pa under 9g forward acceleration

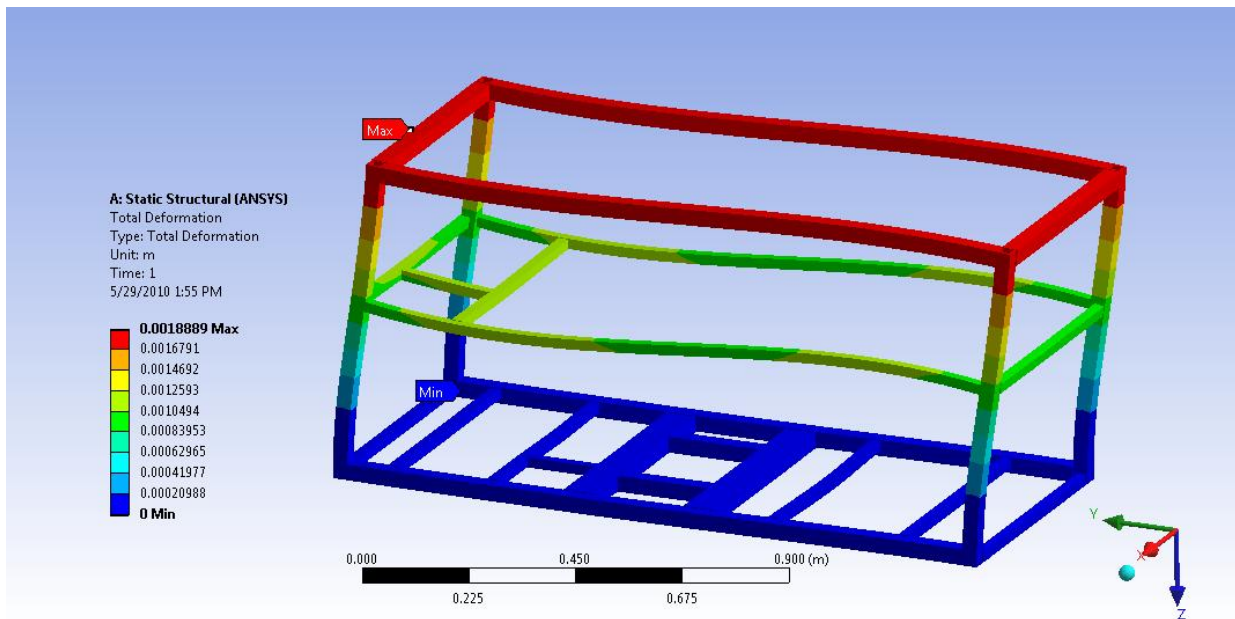


Figure 25: Max deformation of 1.8889e-3 m under 9g forward acceleration

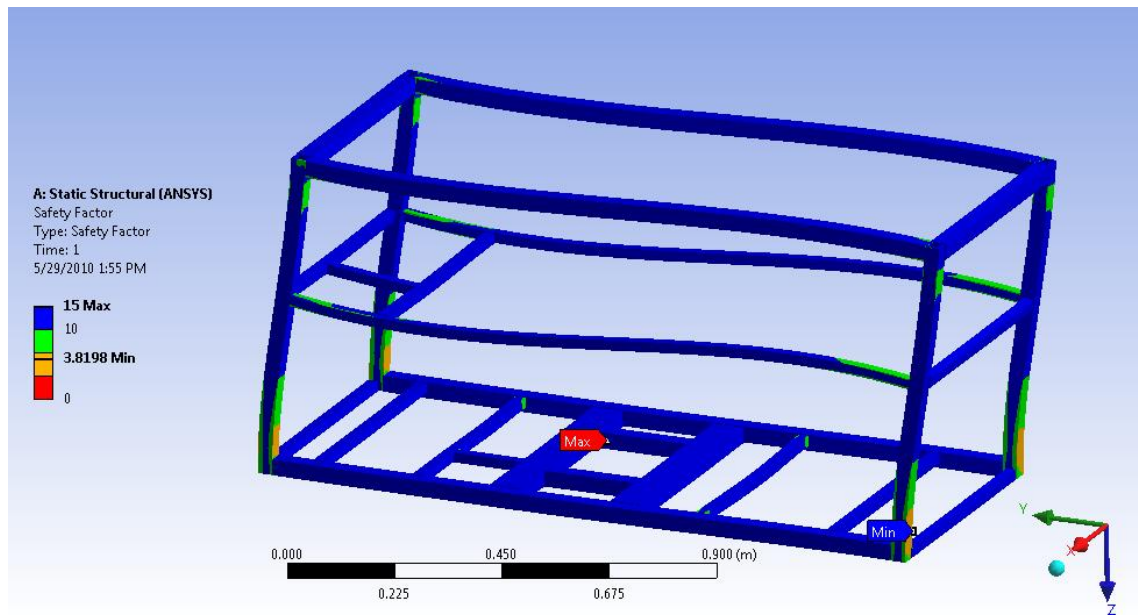


Figure 26: Minimum factor of safety of 3.8198 under 9g forward acceleration

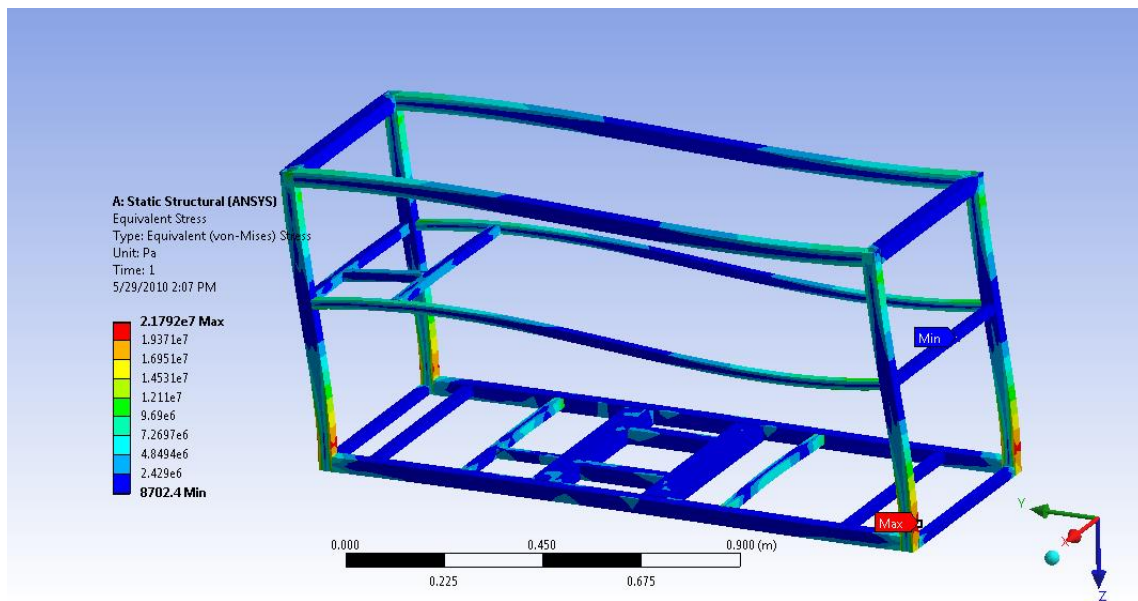


Figure 27: Max stress of 2.192e7 Pa under 3g aft acceleration

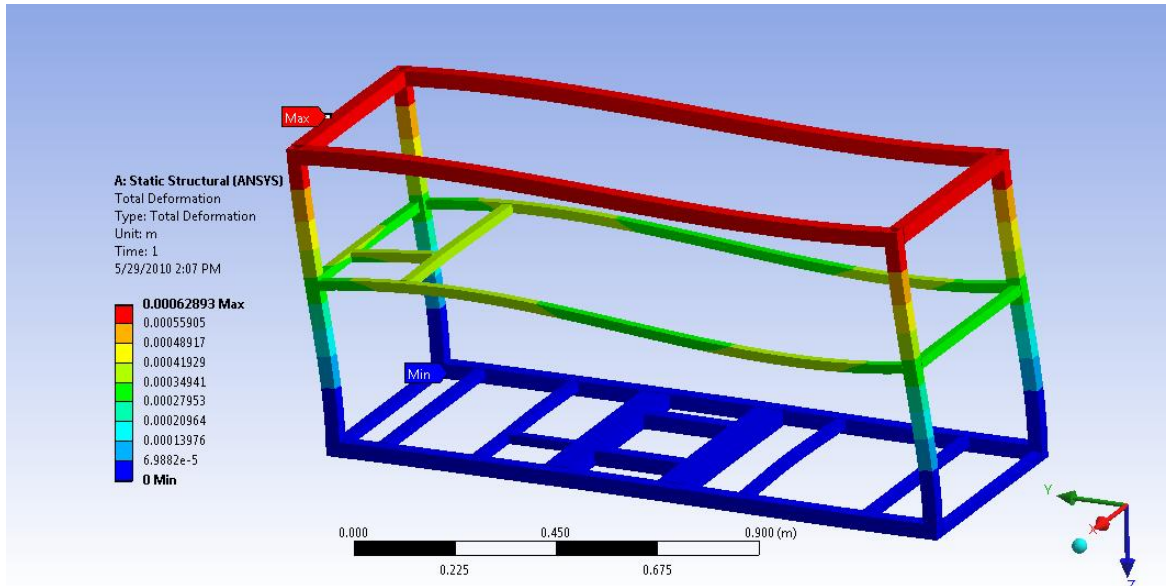


Figure 28: Max deformation of 62893e-4 m under 3g aft acceleration

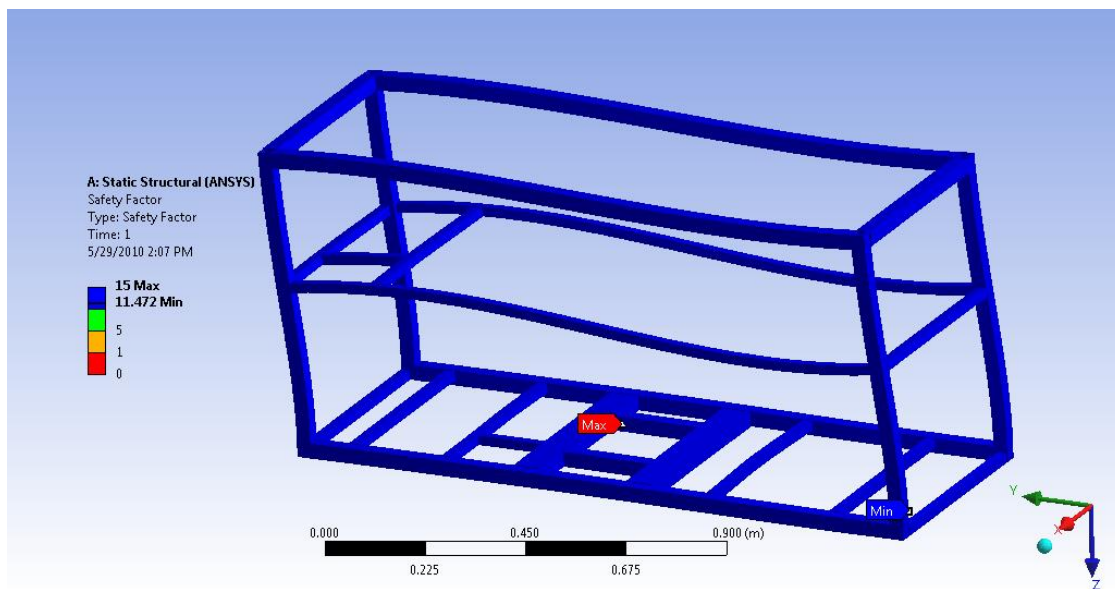


Figure 29: Minimum factor of safety of 11.472 under 3g aft acceleration

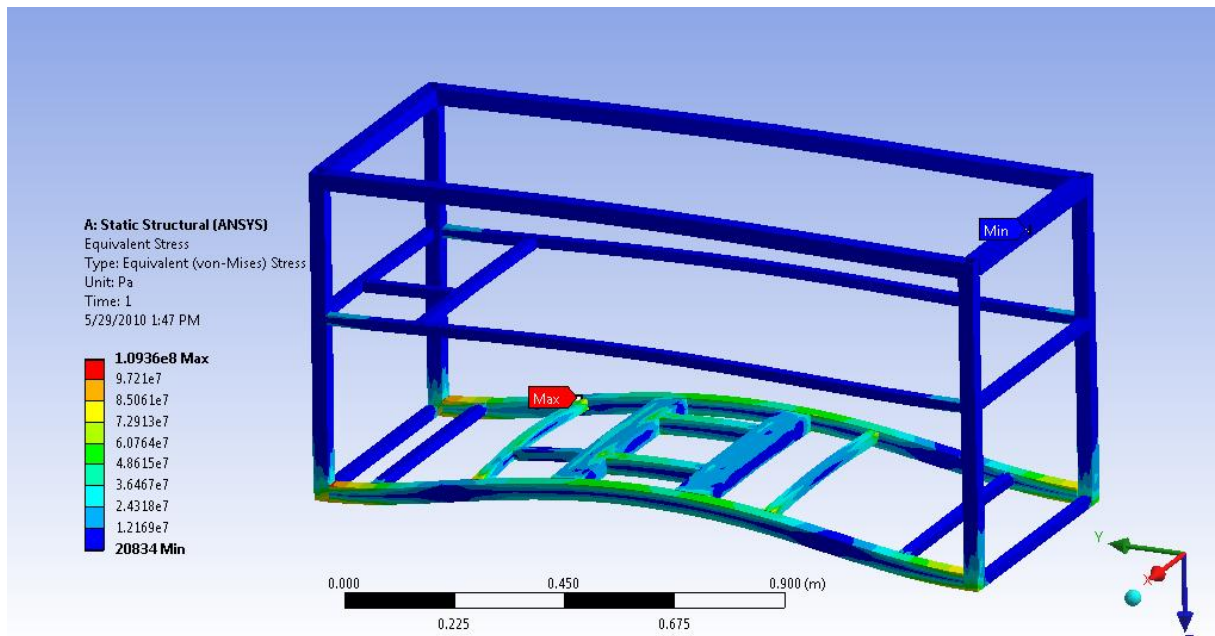


Figure 30: Max stress of 1.0936e8 Pa under 6g downward acceleration

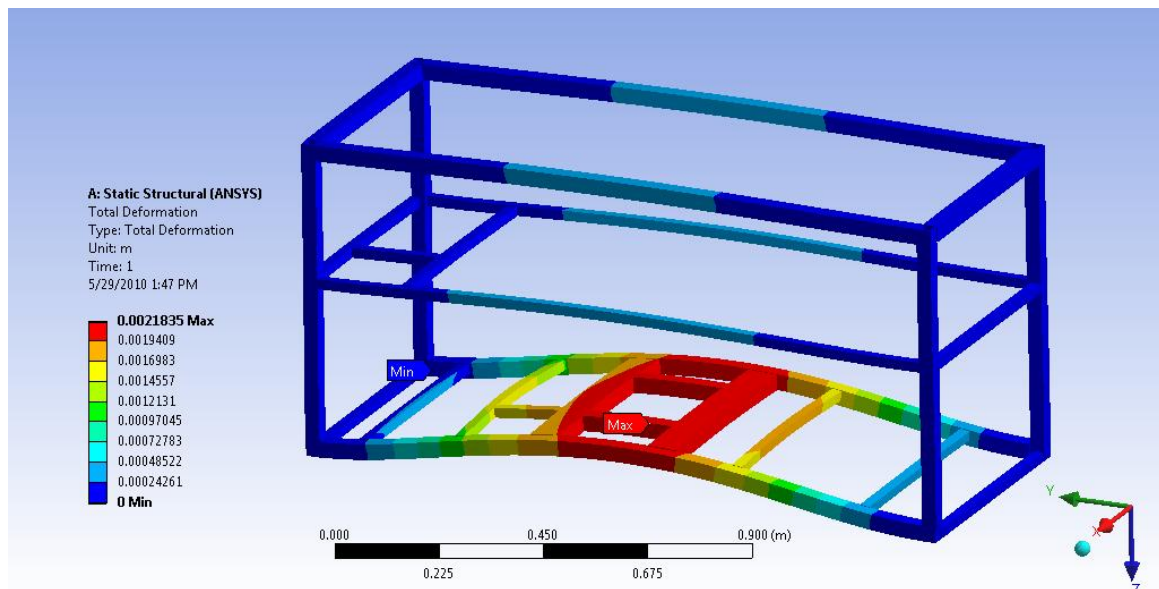


Figure 31: Max deformation of 2.1835e-3 m under 6g downward acceleration

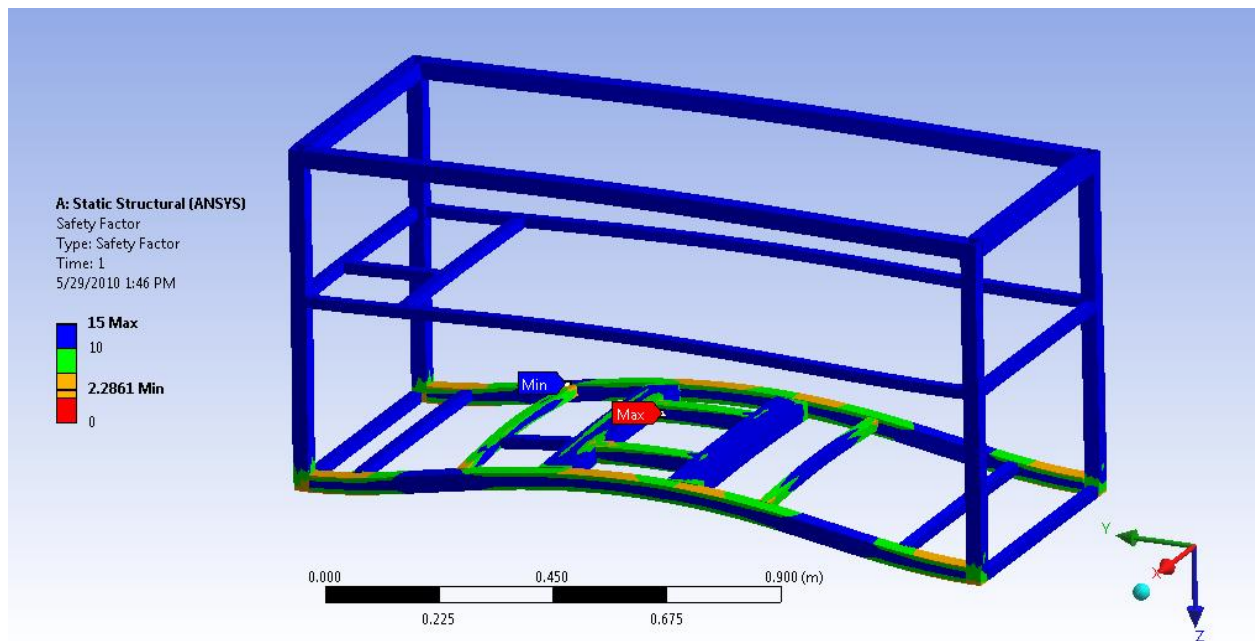


Figure 32: Minimum factor of safety of 2.2861 under 6g downward acceleration

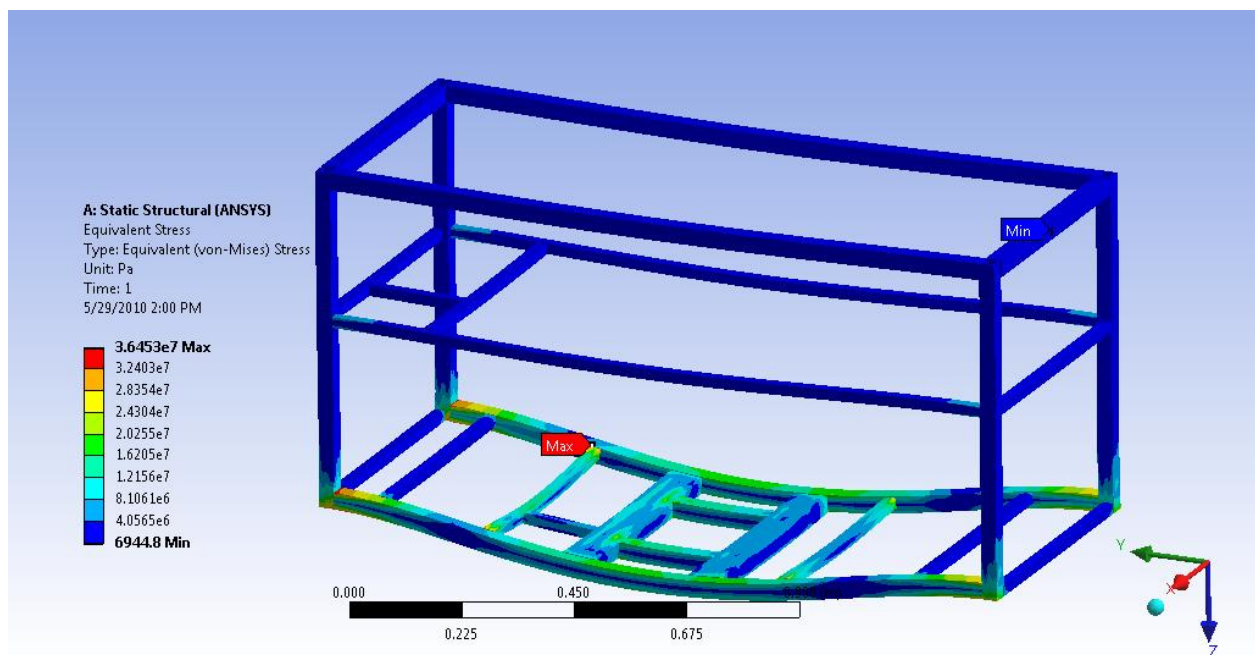


Figure 33: Max stress of 3.6453e7 Pa under 2g upward acceleration

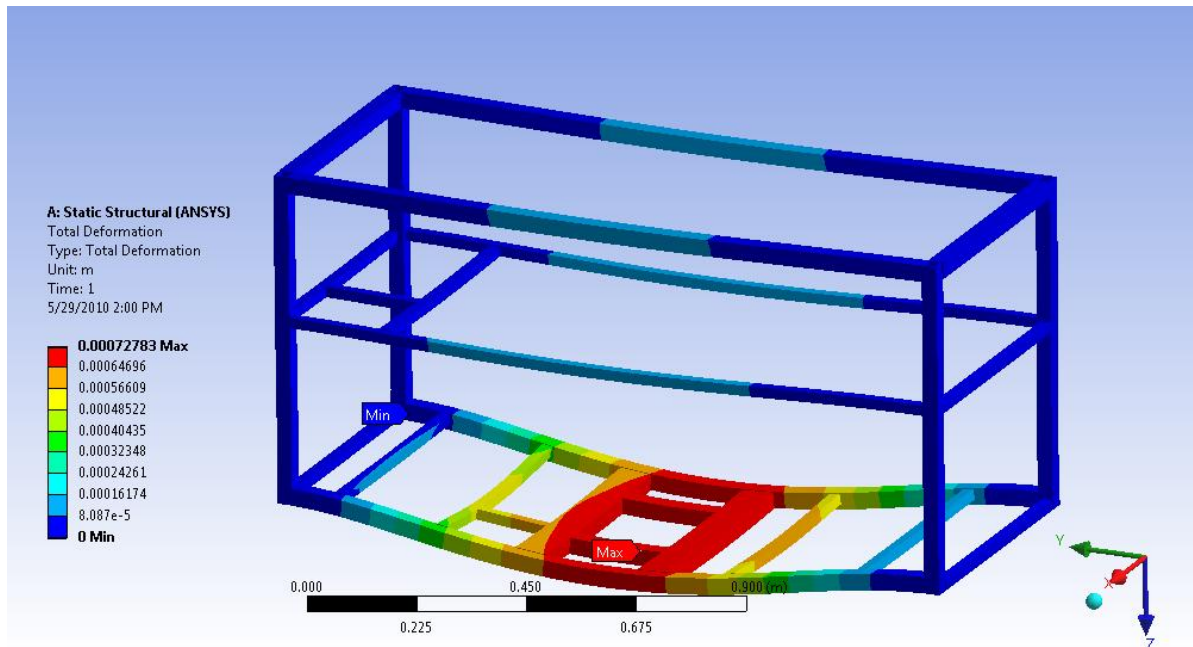


Figure 34: Max deformation of 7.2783e-4 m under 2g upward acceleration

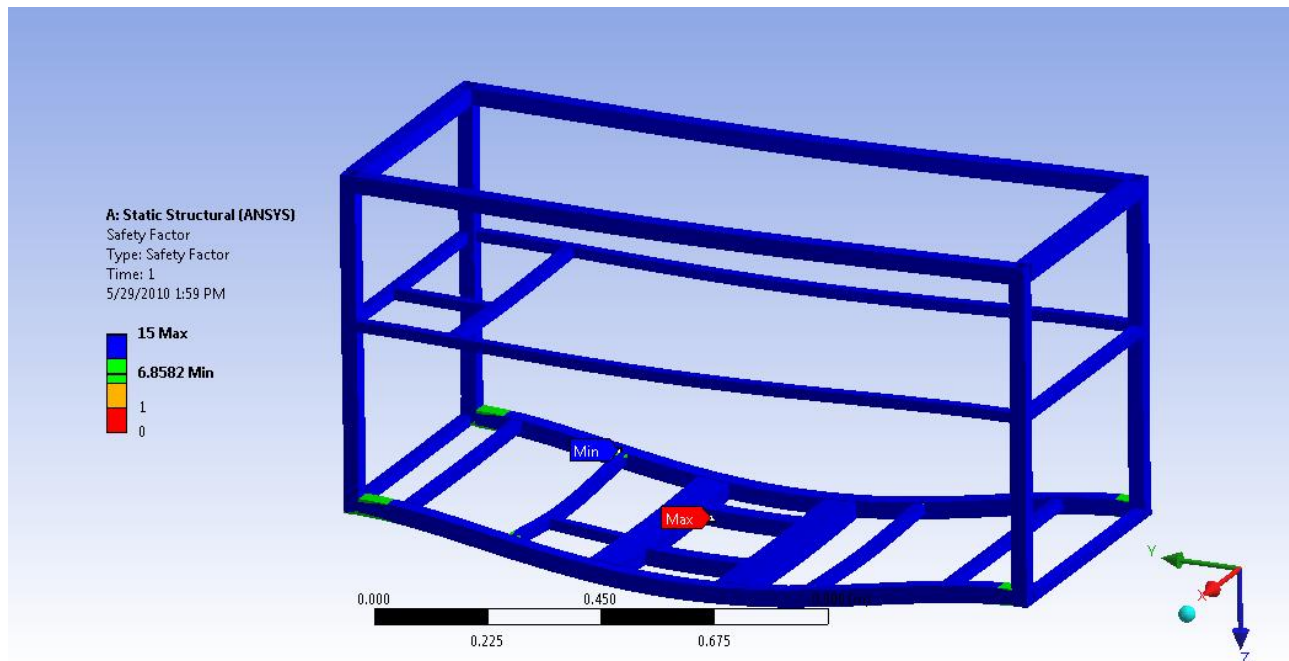


Figure 35: Minimum factor of safety of 6.8582 under 2g upward acceleration

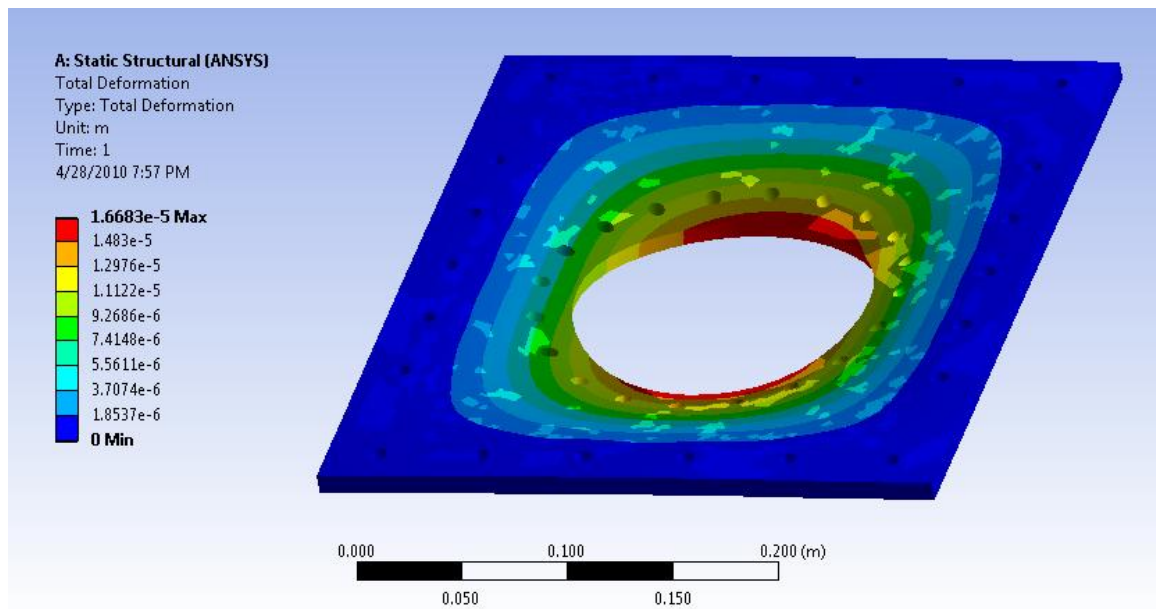


Figure 36: Max deformation of 1.6683e-5 m under 6g down. 8708 Pa distributed pressure

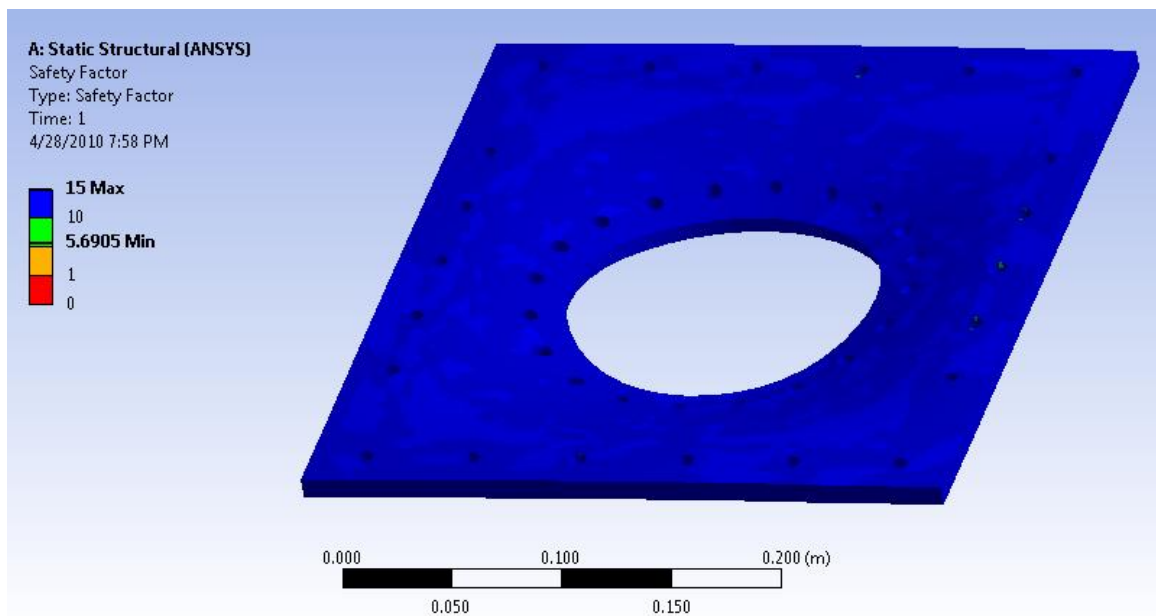


Figure 37: Minimum factor of safety of 5.6905 under 6g down. 8708 Pa distributed pressure

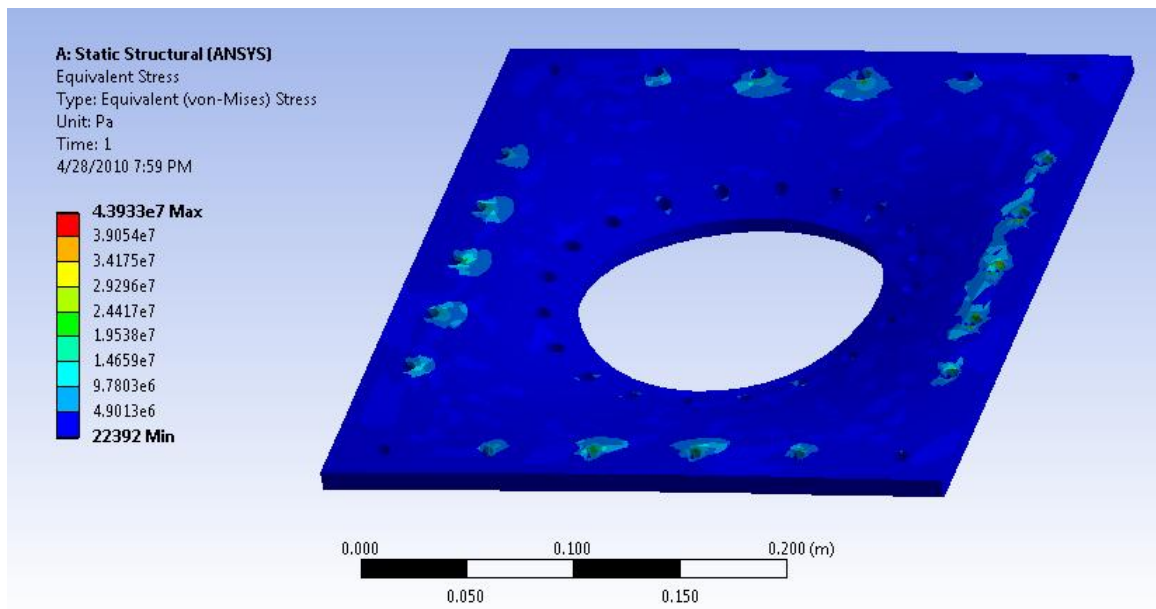


Figure 38: Max stress of 4.393e7 Pa under 6G down. 8708 Pa distributed pressure

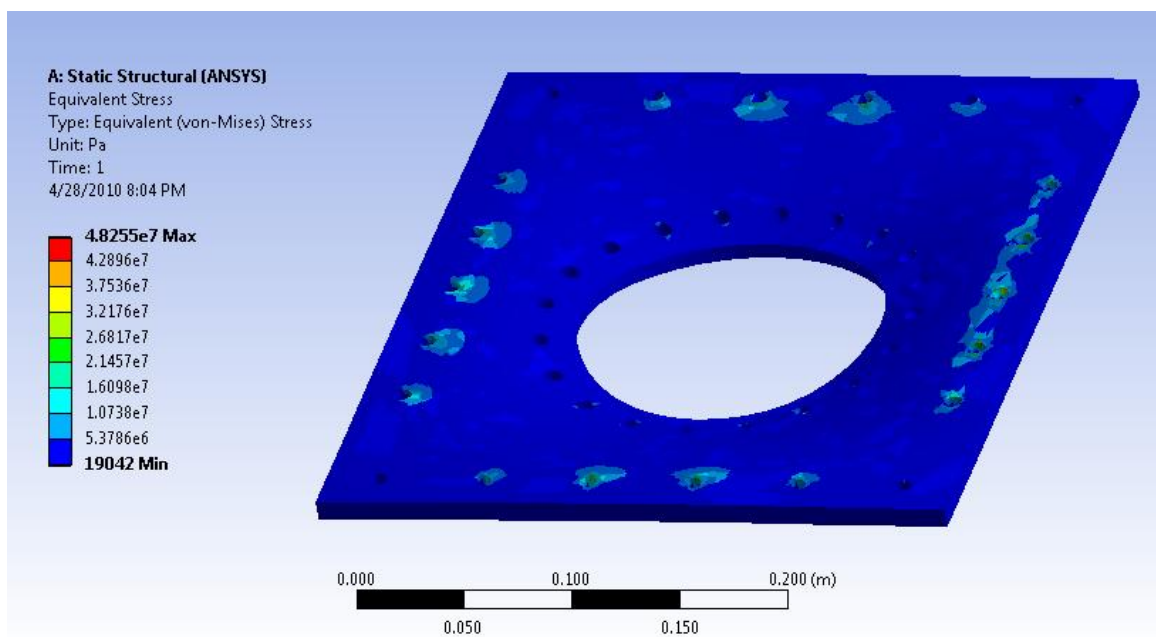


Figure 39: Max stress of 4.8255e7 Pa under 9g forward—worse than 3g lateral

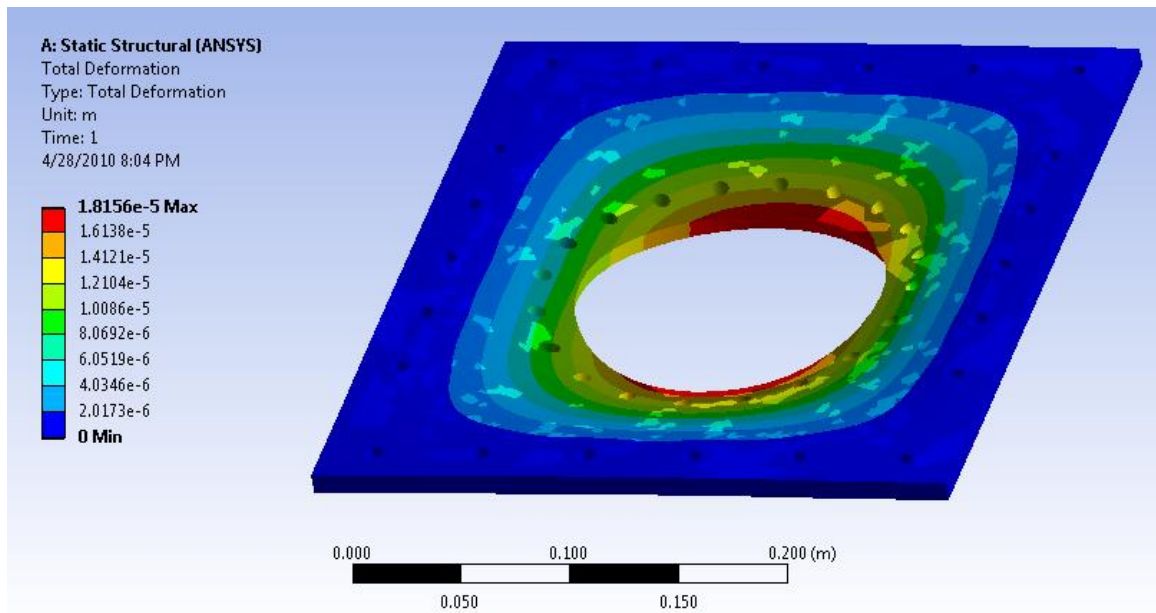


Figure 40: Max deformation of 1.8156e-5 m under 9g forward—worse than 3g lateral

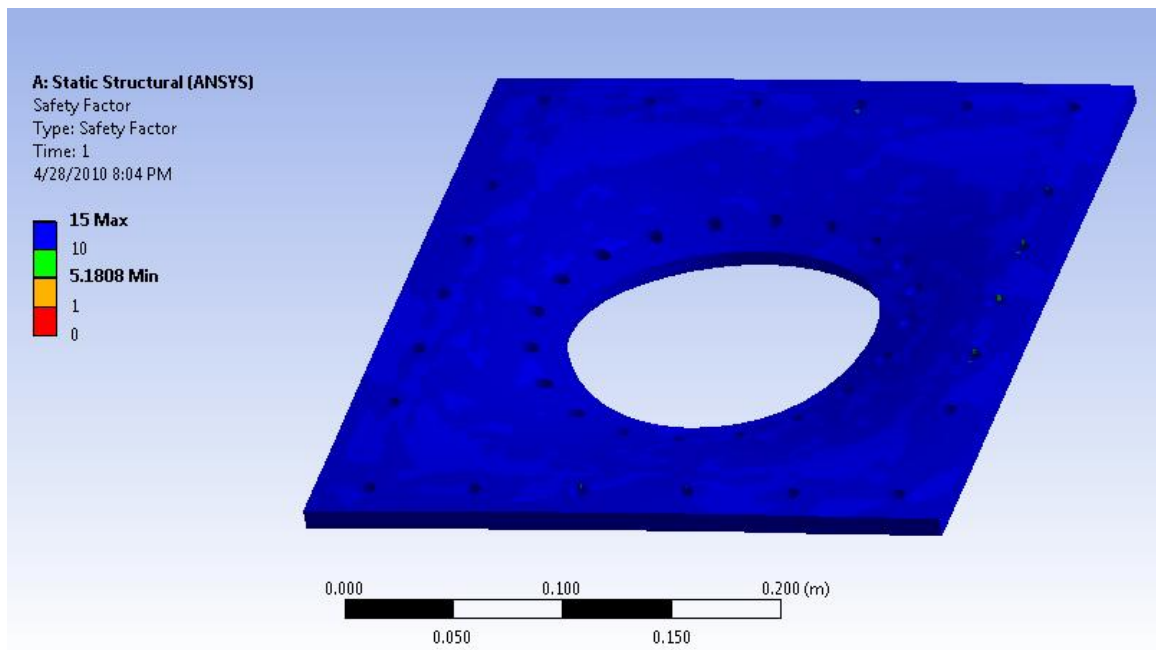


Figure 41: Minimum factor of safety of 5.1808 under 9g forward—worse than 3g lateral

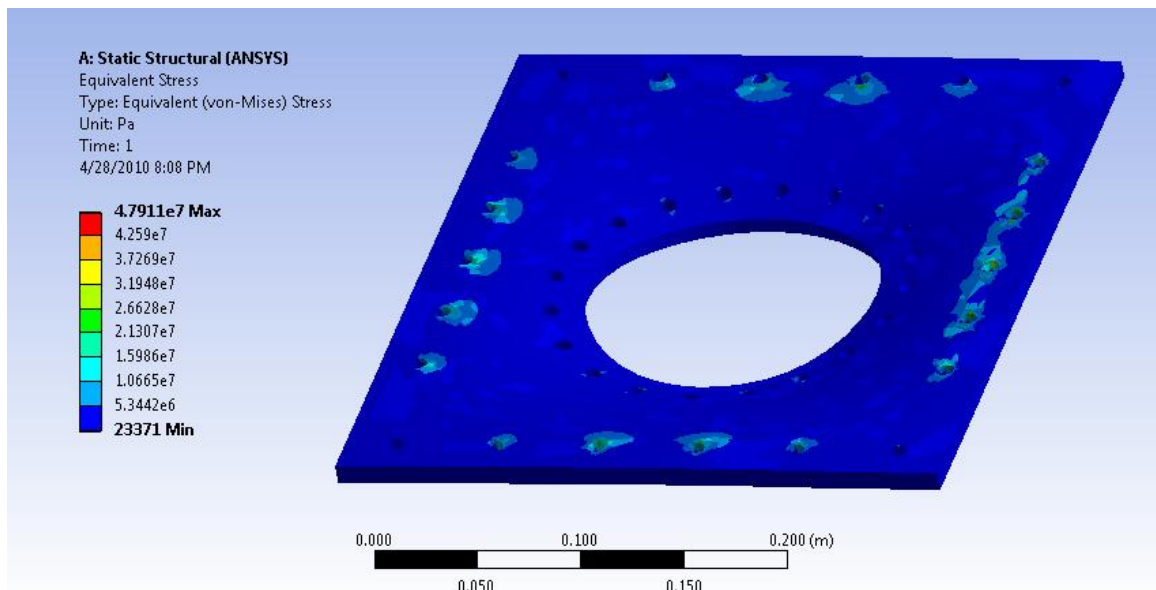


Figure 42: Max stress of 4.7911e7 Pa under 3g aft

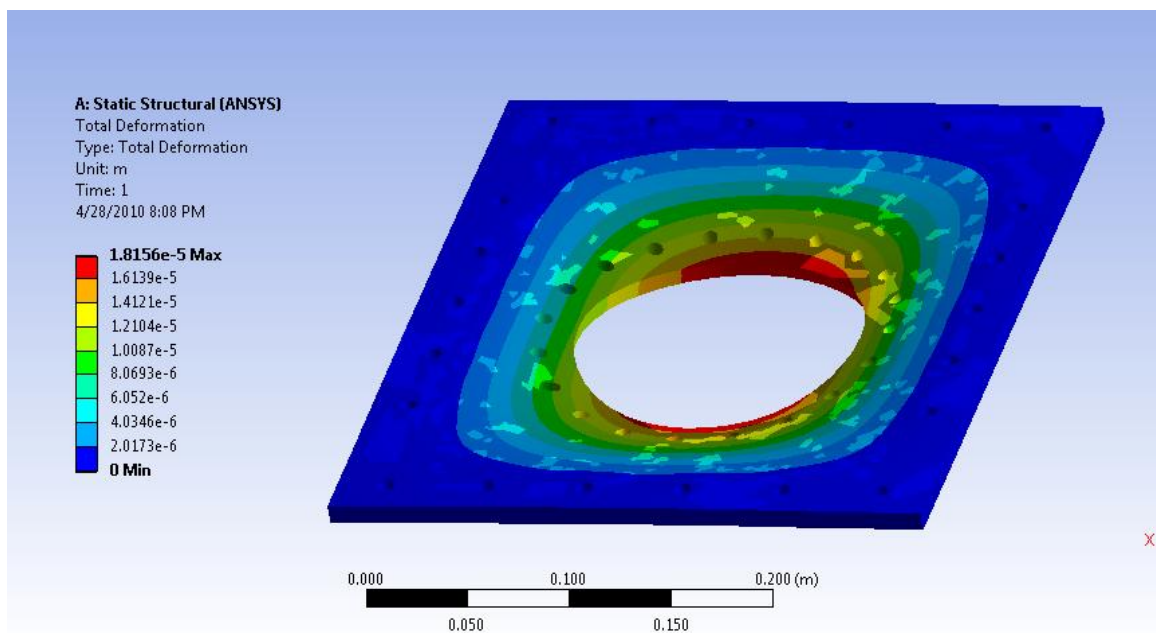


Figure 43: Max deformation of 1.8156e-5 m under 3g aft

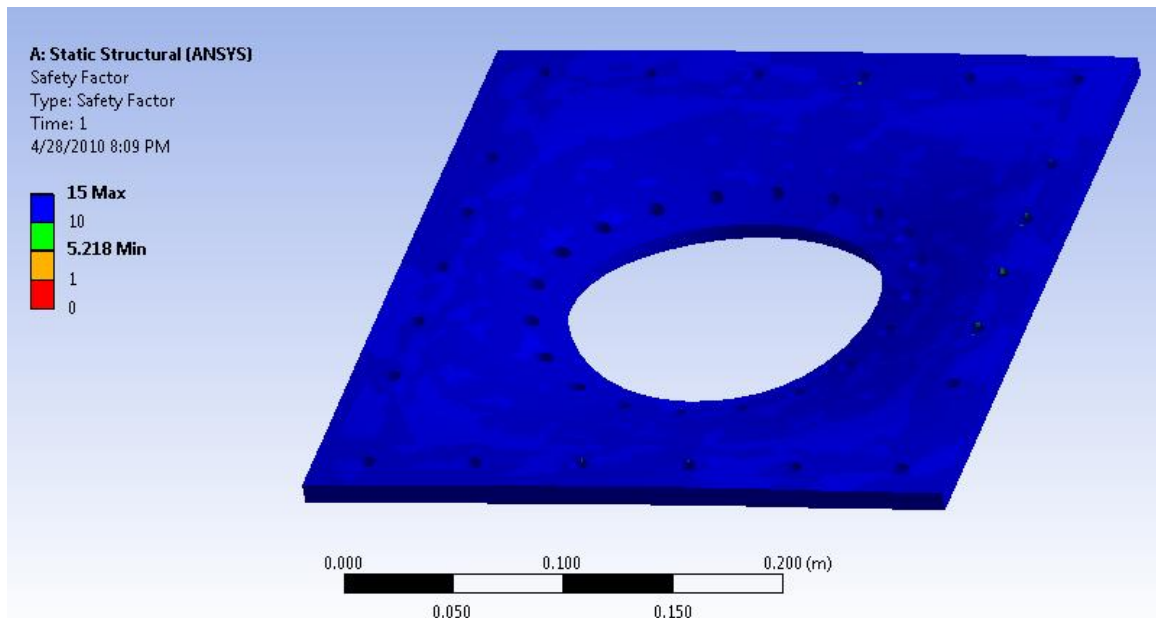


Figure 44: Minimum factor of safety of 5.218 under 3g aft

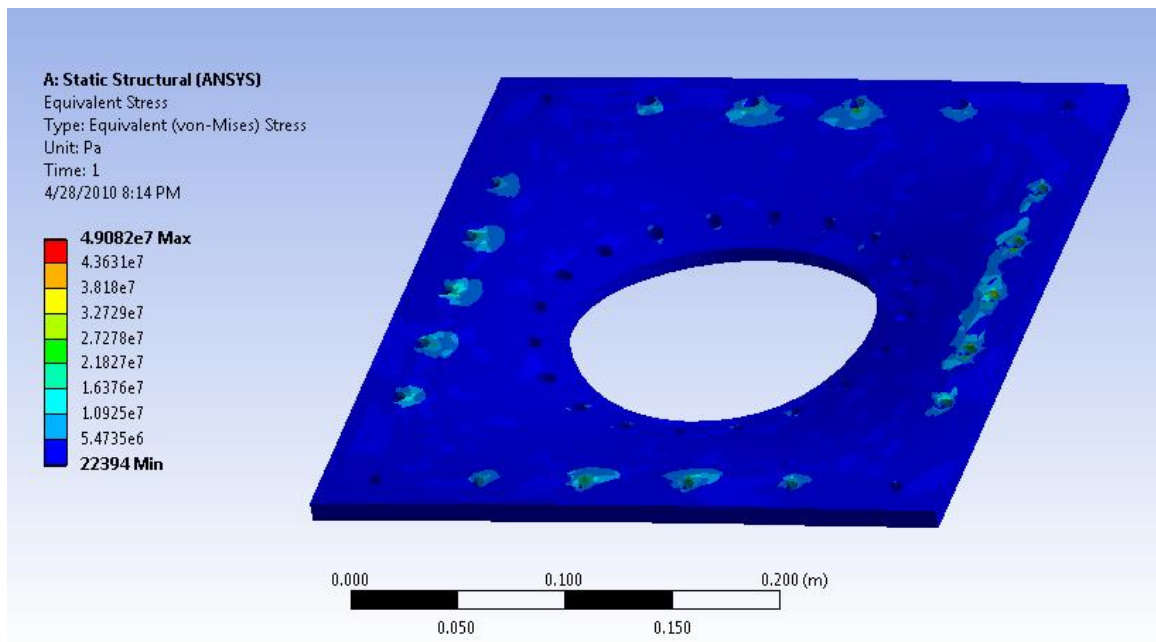


Figure 45: Max stress of 4.9082e7 Pa under 2g up

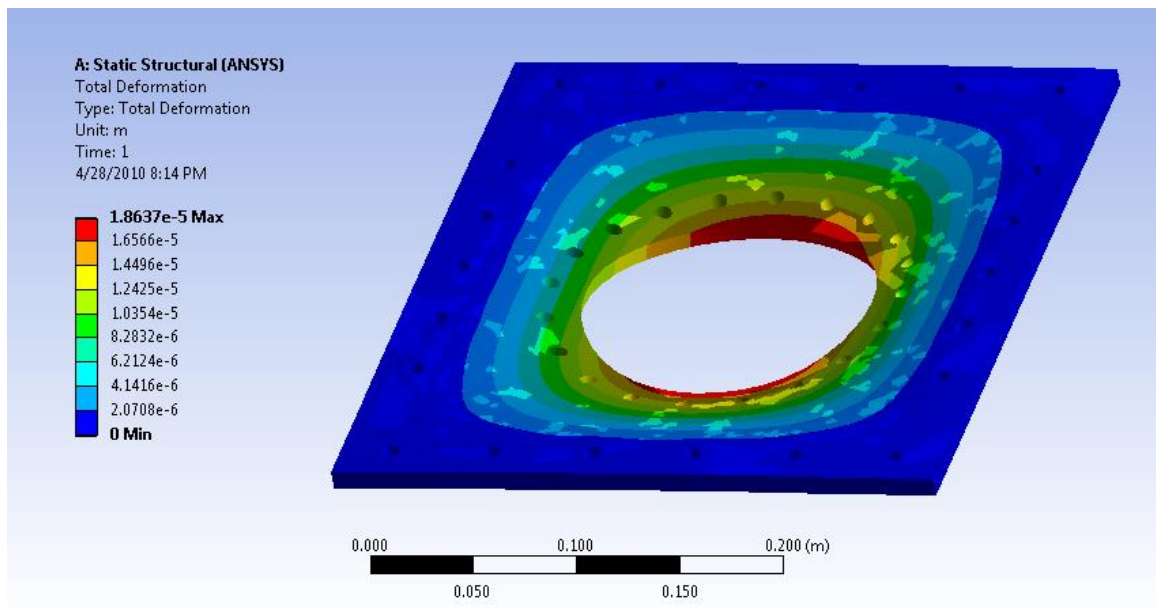


Figure 46: Max deformation of 1.8637e-5 m under 2g up

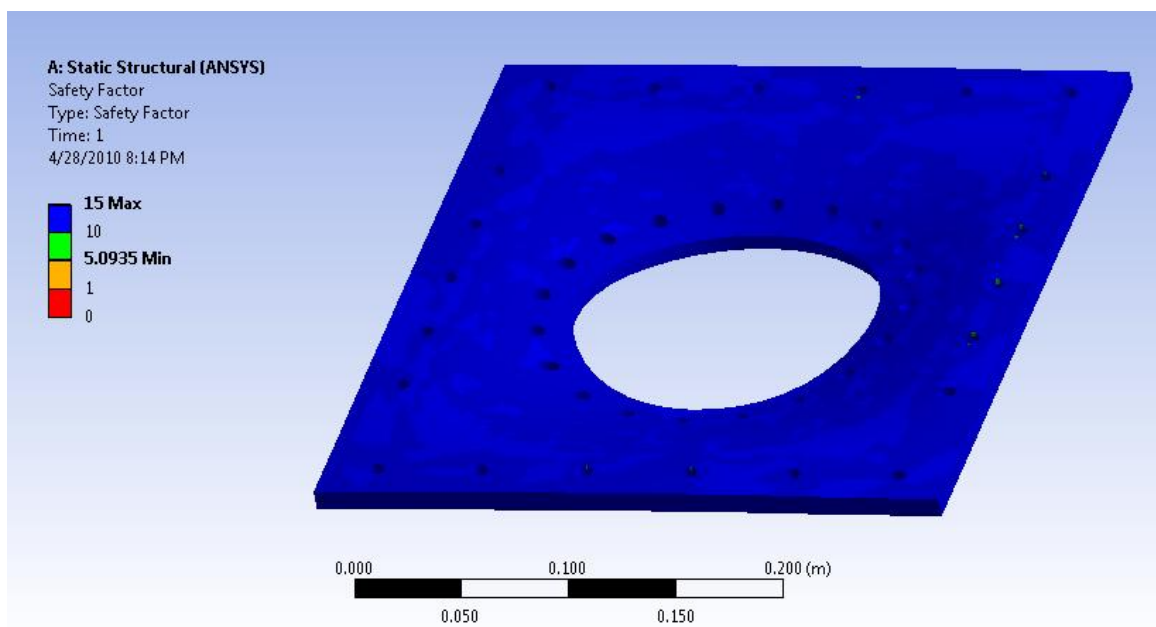


Figure 47: Minimum factor of safety of 5.0935 under 2g up.